



Role of the Tenax® adsorbent in the interpretation of the EGA and GC-MS analyses performed with the Sample Analysis at Mars in Gale crater

Arnaud Buch, Imène Belmahdi, Cyril Szopa, Caroline Freissinet, Daniel P. Glavin, Maeva Millan, Roger Summons, David Coscia, Samuel Teinturier, Jean-Yves Bonnet, et al.

► To cite this version:

Arnaud Buch, Imène Belmahdi, Cyril Szopa, Caroline Freissinet, Daniel P. Glavin, et al.. Role of the Tenax® adsorbent in the interpretation of the EGA and GC-MS analyses performed with the Sample Analysis at Mars in Gale crater. *Journal of Geophysical Research. Planets*, Wiley-Blackwell, 2019, 124 (11), pp.2819-2851. 10.1029/2019JE005973 . insu-02311531

HAL Id: insu-02311531

<https://hal-insu.archives-ouvertes.fr/insu-02311531>

Submitted on 26 Apr 2021

HAL is a multi-disciplinary open access archive for the deposit and dissemination of scientific research documents, whether they are published or not. The documents may come from teaching and research institutions in France or abroad, or from public or private research centers.

L'archive ouverte pluridisciplinaire **HAL**, est destinée au dépôt et à la diffusion de documents scientifiques de niveau recherche, publiés ou non, émanant des établissements d'enseignement et de recherche français ou étrangers, des laboratoires publics ou privés.

Key Points:

- In this article, we evaluate the impact of the Tenax® traps on the Sample Analysis at Mars experiment results, with concurrent implications for the future Martian Organic Molecule Analyser experiment results
- Tenax® is an adsorbent resin used on SAM as a trap; it is an organic polymer that can be degraded into smaller molecules
- By-products of Tenax® may contribute to the background of the SAM chromatogram. Here we identify them and the conditions of their production

Correspondence to:

A. Buch,
 arnaud.buch@centralesupelec.fr

Citation:

Buch, A., Belmahdi, I., Szopa, C., Freissinet, C., Glavin, D. P., Millan, M., et al. (2019). Role of the Tenax® adsorbent in the interpretation of the EGA and GC-MS analyses performed with the Sample Analysis at Mars in Gale crater. *Journal of Geophysical Research: Planets*, 124, 2819–2851. <https://doi.org/10.1029/2019JE005973>

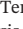






Received 26 MAR 2019

Accepted 10 SEP 2019

Accepted article online 10 OCT 2019

Published online 11 NOV 2019

Role of the Tenax® Adsorbent in the Interpretation of the EGA and GC-MS Analyses Performed With the Sample Analysis at Mars in Gale Crater

A. Buch¹ , I. Belmahdi¹, C. Szopa^{2,3}, C. Freissinet², D.P. Glavin⁴ , M. Millan^{4,5}, R. Summons⁶ , D. Coscia², S. Teinturier⁴, J.-Y. Bonnet², Y. He¹, M. Cabane², R. Navarro-Gonzalez⁷ , C.A. Malespin⁴, J. Stern⁴ , J. Eigenbrode⁴ , P.R. Mahaffy⁴ , and S.S. Johnson⁵

¹Laboratoire Génie des Procédés et Matériaux, CentraleSupélec, Gif-sur-Yvette, France, ²LATMOS/IPSL, UVSQ Université Paris-Saclay, Sorbonne Université, CNRS, Guyancourt, France, ³Institut Universitaire de France, Paris, France, ⁴NASA Goddard Space Flight Center, Greenbelt, MD, USA, ⁵Department of Biology, Georgetown University, Washington, DC, USA, ⁶IMT, Cambridge, MA, USA, ⁷Instituto de Ciencias Nucleares, Universidad Nacional Autónoma de México, Circuito Exterior, Ciudad Universitaria, Ciudad de México, Mexico

Abstract The Sample Analysis at Mars (SAM) experiment on the National Aeronautics and Space Administration Curiosity rover seeks evidence of organic compounds on the surface of Mars. Since the beginning of the mission, various organic molecules have been detected and identified. While several have been demonstrated to be indigenous to the Martian soil and rocks analyzed, others appear to have been produced from sources internal to the experiment. The objective of this study is to build an exhaustive molecular database to support the interpretation of SAM results by identifying all the chemical species produced from Tenax® adsorbents, by determining (1) the thermal degradation by-products of Tenax®, (2) the effect of Tenax® conditioning on the formation of Tenax® by-products, (3) the impact of MTBSTFA or a mixture of MTBSTFA and DMF on Tenax® decomposition, and (4) the reaction between Tenax® and calcium perchlorate. Our results indicate that the by-products of the SAM trap are due to the impact of trap heating, the impact of the derivatization reagent (MTBSTFA) and the presence of perchlorate in Martian soil. Some of these by-products are observed in the SAM gas chromatograph mass spectrometer data from Mars.

Plain Language Summary The Sample Analysis at Mars (SAM) experiment onboard the Curiosity Rover has a polymer-based chemical trap (Tenax®) that concentrates the evolved species from the Martian samples. We studied the impact that this trap could have on the SAM results when heated, when exposed to the chemical compounds used for sample processing (derivatization) and when exposed to Martian perchlorates. We conclude by demonstrating that some of the organic compounds detected in the background signal of the SAM chromatograms likely came from the degradation of Tenax®. This study will help to discriminate the endogenous organic compounds detected on Mars by SAM from the contamination.

1. Introduction

1.1. The Quest for Organics on Mars

The search for organics on Mars is key in the distribution of the organic matter in the solar system, understanding the emergence of life, and potentially discovering the presence of life on Mars. The Viking, Phoenix, and Mars Science Laboratory (MSL) missions have focused on these objectives. The Viking lander was the first successful spacecraft to reach the Martian surface in the summer of 1976. The gas chromatograph-mass spectrometer (GC-MS) experiment onboard was devoted to characterizing the organic material (OM) present in solid samples acquired by the lander (Biemann et al., 1976). It was capable of volatilizing or thermally degrading organic compounds from Martian soil samples by heating them up to 500 °C in dedicated ovens. The volatile molecules released from the samples were then analyzed by GC-MS for detection and identification. The Viking GC-MS analyses reveal the presence of acetone, freon-E, benzene, toluene, xylene, methylfluorosiloxane, chloromethane, and dichloromethane (Biemann et al., 1977). The origin of these compounds was first proposed to be terrestrial contamination; for instance, the

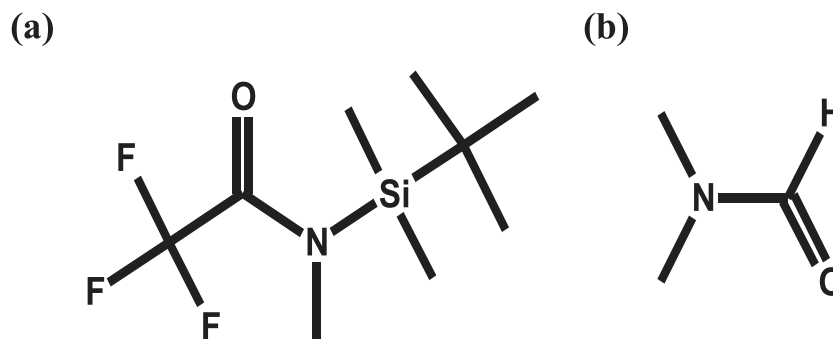


Figure 1. Chemical diagram of (a) *N*-tert-butyltrimethylsilyl-*N*-methyltrifluoroacetamide (MTBSTFA) and (b) dimethylformamide (DMF).

dichloromethane was widely attributed to residues of solvents used for cleaning procedure (NASW-4355, 1988). However, the possibility that chloromethane could originate on Mars could not be excluded (Biemann et al., 1977). Decades later, with the discovery of perchlorates (0.4 to 0.6 wt%) in Martian soil with the Phoenix mission (Hecht et al., 2009), results have been reinterpreted after showing that heating a mixture of organic molecules and perchlorates under the GC-MS experimental conditions produced chloromethane and other chlorine-bearing organics (Navarro-Gonzalez et al., 2010). Perchlorates were also recently detected with the Sample Analysis at Mars (SAM) experiment on the Curiosity rover in soil samples in Gale crater (Glavin et al., 2013). This detection, in a quite different region than the high latitude northern plains where the Phoenix probe landed, adds to models of production of perchlorates on Mars (Carrier & Kounaves, 2015; Clark & Kounaves, 2016) and suggests that perchlorates could be widespread at the surface of Mars. It is possible that the chlorohydrocarbons detected with the GC-MS experiment onboard Viking were representative of organics indigenous to the samples that would have reacted with perchlorates. But this assumption cannot be verified by the limited number of experiments carried out with Viking's GC-MS experiment. But more recently it has been suggested that the presence of chlorobenzene in the Viking signal could have been the result of a reaction of Martian organic molecules with Martian perchlorate (Guzman et al., 2018).

Since Viking, we have made substantial strides in our ability to detect OMs on the surface of Mars. The MSL is capable of detecting a wide range of organic molecules, including the carboxylic salts, after derivatization, predicted by Benner et al. (2000). The SAM Sample Acquisition/Sample Processing and Handling system (SA/SpaH) can receive Martian scooped soil or drilled rock samples. Each sample is placed in one of 74 cups that can be heated up to ~900 °C. There are six calibration cups and 68 sample cups, including 59 empty quartz cups for pyrolysis and nine metal cups containing wet chemistry solvent (seven with *N*-(*tert*-butyldimethylsilyl)-*N*-methyl-trifluoroacetamide (MTBSTFA) and dimethylformamide (DMF) 4:1 for derivatization experiments (Figures 1a and 1b) and two with tetramethylammonium hydroxide (TMAH) diluted in methanol (25% v/v) for thermochemolysis experiments).

SAM uses two sample preparation modes: pyrolysis and wet chemistry (derivatization and thermochemolysis). Pyrolysis consists of exposing the samples to high temperatures (up to 800 °C; Moldoveanu, 1998). The aim of the wet chemistry experiments is to increase the range of compounds analyzable by GC-MS by reducing the polarity of the OM contained in the sample. Due to the polar nature of several Martian molecular targets (amino acids, carboxylic acids, amines, *etc.*), derivatization is required in order to make analytes less polar, less reactive by reducing their ability to do intermolecular and intramolecular H-bonding, and thus more volatile (Lin et al., 2008; Orata, 2012), improving their thermal stability and their chromatographic analysis. MTBSTFA is a silyl reagent (Figure 1), which replaces any labile (reactive) hydrogen in chemical bonds (e.g., -OH, -NH₂, -SH, and -COOH) with the nonpolar moiety -Si (CH₃)₂C(CH₃)₃ (Kataoka, 1996). Thermochemolysis thermally degrades molecules before the substitution of acidic hydrogen by apolar groups from TMAH (i.e., methyl groups -CH₃; Challinor, 2001; Gallois et al., 2010; Shadkani & Helleur, 2010).

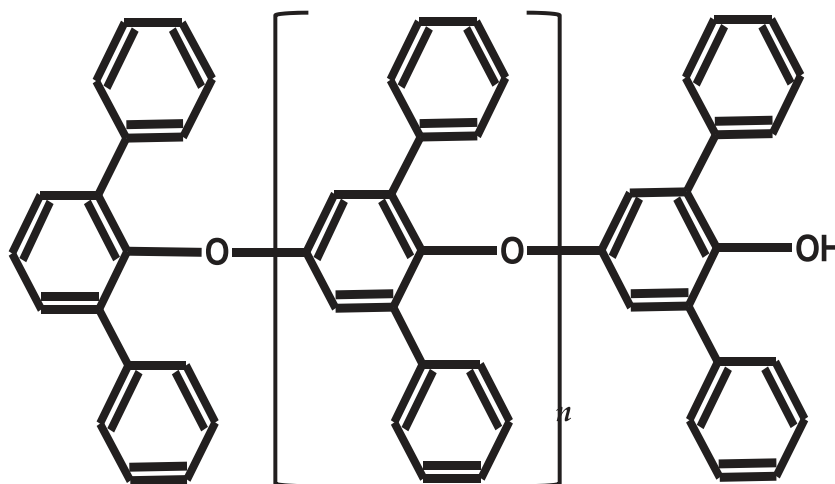


Figure 2. Chemical formula of poly(2,6-diphenylphenylene oxide) polymer.

After sample preparation, the stream of helium is divided: a 1:800 fraction is sent directly to the quadrupole mass spectrometer, while the sample is heated at a rate of 35 °C/min (evolved gas analysis modes). The fraction sent to GC-MS is first trapped on the hydrocarbon (HC) trap and then the injector trap (IT), which serves to preconcentrate the chemical compounds before a pulsed thermal injection into the column for analysis (GC-MS mode). The HC trap is packed with three types of adsorbents in series: nonporous silica beads, Tenax[®] TA, and 60/80 mesh Carbosieve G (Mahaffy et al., 2012), whereas the IT in front of GC Column 5, the most commonly used column on SAM to date, is packed with Tenax[®] GR (Mahaffy et al., 2012). Tenax[®] TA is a porous polymer made of poly(2,6-diphenyl-p-phenylene oxide) polymer (PPPO; Figure 2), and Tenax[®] GR is made of 70% of PPPO and 30% graphitic carbon, which are respectively used to trap C₆-C₂₆ and C₇-C₃₀ organic molecules.

1.2. SAM Objectives and Results

Among SAM's objectives is the search for indigenous organic compounds in Mars' subsurface (down to 6-cm maximum; Mahaffy et al., 2012). Organic molecules indigenous to a Martian sample were identified early in the mission. These include chlorobenzene (if generated *in situ* under Martian irradiation; Freissinet et al., 2015) and dichlorobenzene (Szopa et al., 2015) as well as C₂ to C₄ dichloroalkanes. The chlorinated aromatic HCs (chlorobenzene and dichlorobenzene) could be either present as is in the Martian sample or more likely derived from other precursors.

The nature of these precursors has been investigated, and possibilities that have been proposed include aliphatic compounds, aryl molecules, and high molecular weight compounds (e.g., kerogen; Freissinet et al., 2015). Experiment showed that acetic acid, propane, propanol, and hexane pyrolyzed with calcium perchlorates generate several chlorine-bearing aliphatic molecules (e.g., 2,3-dichlorobutane, chlorohexane, dichlorohexane, 2-chloropropane, 1,2,3-trichloropropane, and 1-chloro-2-propanone), some of which are detected by SAM, that is, dichloromethane, carbon tetrachloride, and 1,2-dichloropropane (Miller et al., 2016). And, pyrolysis of Murchison kerogen in the presence of calcium perchlorate releases chloromethane, chloroethane, chloropropane, and chlorobenzene (Miller et al., 2016). All of them have been detected by SAM (Freissinet et al., 2015).

Some authors also demonstrated that functionalized aromatic compounds, that is, benzoic acid, phthalic acid, and mellitic acid, can be precursors of chlorobenzene and dichlorobenzene when they are mixed with perchlorates and chloride (Miller et al., 2016; Steininger et al., 2012). It has been suggested that the benzenecarboxylic acid family of compounds are metastable products of the oxidation of aromatic HCs and acid insoluble kerogens by hydroxide radical (photodissociation product of water by UV radiation; Benner et al., 2000). However, other sources of organic matter transformation exist, including radiation and other oxidants. For instance, Stalport et al. studied the effect of UV radiation on benzenecarboxylic acids and oxalic acid. He

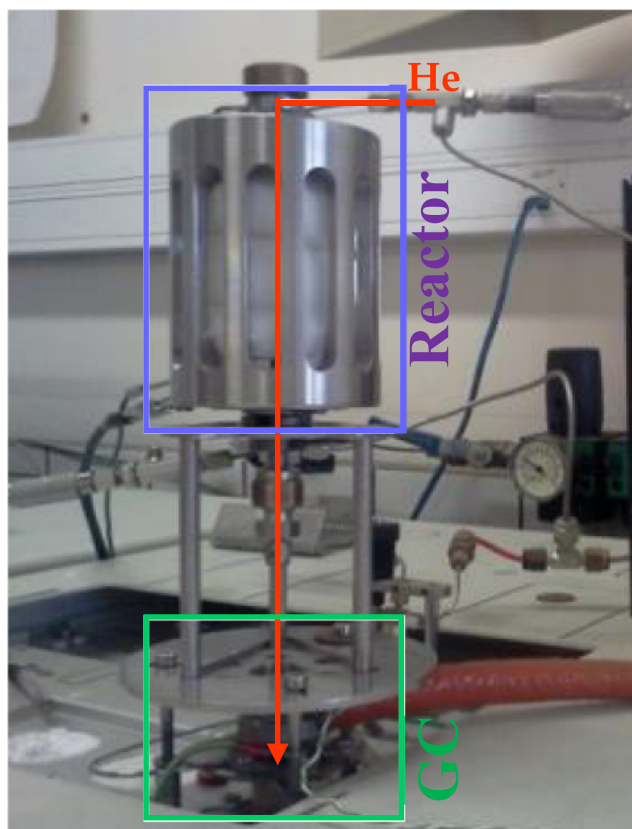


Figure 3. Sample preparation device (Buch, Sternberg, & Chazalnoel, 2009). The reactor is 20 cm high and has a diameter of 7 cm. It consists of a gas chromatograph liner that can be used in split or splitless mode. It can go from a temperature of +20 to +600 °C in 30 s. The reactor can also be quickly cooled with liquid CO₂, from 600 to −180 °C in 30 s. A septum makes it possible to carry out injections through gas chromatograph syringes.

demonstrated that benzoic acid, oxalic acid, phthalic acid, and trimesic acid are rapidly destroyed by such radiation (Stalport et al., 2009; Stalport et al., 2010). Only mellitic acid persists after evolving into an UV and oxidation resistant compound (benzenehexacarboxylic acid-trianhydride (C₁₂O₉)) (Poch et al., 2014; Stalport et al., 2009).

Several other organic molecules have been identified as part of the SAM GC-MS background: compounds released by the stationary phase of the column; residues of preflight tests; residues of MTBSTFA and DMF; nonchlorinated aromatic compounds from Tenax[®] degradation; permanent gases from the degradation of MTBSTFA, DMF, and Tenax[®]; and mineral thermal degradation products. Among those molecules, phenol, a functionalized aromatic, is known to be released from the Tenax[®] trap and could sustain chlorination from the perchlorates of the sample. Additionally, SAM has also identified various chlorination states of methane, thought to be a product of perchlorate-mediated chlorination of methane from MTBSTFA degradation (Glavin et al., 2013), although a Martian origin of the methane cannot be excluded (Webster et al., 2018).

MTBSTFA and DMF by-products are very well known (Freissinet et al., 2015; Glavin et al., 2013; Miller et al., 2016), but this is not the case of Tenax[®] within SAM conditions. Because Tenax[®] is an organic polymer, it is able to generate by-products when it is heated or exposed to reactive gas such as NO₂ or O₃ (Clausen & Wolkoff, 1997; Klenø et al., 2002). The main degradation products of Tenax[®] are 2,6-diphenyl-p-benzoquinone, 2,6-diphenyl-p-hydroquinone, and acetophenone.

Moreover, the Tenax[®] adsorbent may be impacted by the storage condition and to the number of times the adsorbent is reused. For example, experiments showed that after a storage of toluene at −20 for 24 hr in a Tenax[®] TA trap, the efficiency of the desorption was decreased by about 10% (Chu et al., 2016).

The objective of this work is to build an exhaustive molecular database to support the interpretation of the SAM results by identifying all the possible sources of contamination brought by the trap adsorbents, especially Tenax[®], and understand modes for their production under SAM conditions. Upon heating, the adsorbents, especially Tenax[®], generate by-products, so it is necessary to determine the nature of these molecules. For this purpose, we tested (1) the thermal stability of Tenax[®] (TA and GR) up to 600 °C and the OM released during their degradation, (2) the impact of MTBSTFA or a mixture MTBSTFA/DMF on the Tenax[®] degradation, and (3) the reactivity between Tenax[®] and calcium perchlorate.

1.3. ExoMars and the Future MOMA Experiments

In 2020, the joint ESA-Roscosmos ExoMars-2020 mission will be launched, including the Mars Organic Molecules Analyser (MOMA) experiment carried by the Rosalind Franklin rover. The goals of the mission include the search for molecules relevant to life on the Martian surface and near subsurface (large, nonvolatile organic or biological molecules that suggest existing or prior biosynthetic activity), as well as the discrimination of endogenous from exogenous sources of organics on Mars. The MOMA experiment will be a key analytical tool in providing chemical (molecular) information from the solid samples collected by the rover, with a particular focus on the characterization of the organic content (Goetz et al., 2016). The MOMA instrument contains a UV laser desorption/ionization ion trap mass spectrometer (LD-ITMS) and a gas chromatograph-ion trap mass spectrometer (GC-ITMS), with on-board derivatization capabilities, which provide the unique capability of characterizing a broad range of compounds, including a range of volatile and nonvolatile species, as well as chiral analysis. Core samples will be extracted as deep as 2 m below the Martian surface to minimize the effects of radiation and oxidation on OMs. Samples will be crushed and deposited into sample cups seated in a rotating carousel. These cups are sealed with a tapping station and gas processing system prior to pyrolysis.

Soil samples will be analyzed either by LDI-ITMS or pyrolysis GC-ITMS. In a subset of GC-MS analyses, select samples are subjected to in situ derivatization, consisting of the reaction of the sample components with specific reactants (MTBSTFA (Buch, Sternberg, Szopa, et al., 2009), DMF-DMA (Freissinet et al., 2010), and TMAH (Geffroy-Rodier et al., 2009)). To preconcentrate the volatile species, two Tenax[®] TA traps will be used (Goesmann et al., 2017). Those traps will be subject to a heating process up to 350 °C in presence of perchlorate salts and a derivatizing reagent (in particular MTBSTFA). Thus, the results of this study will not only impact our understanding of the SAM results from Gale Crater but also help to interpret the future GC-MS data from the ExoMars mission.

2. Materials and Methods

2.1. Reagents and Materials

The physical thermal evolution of Tenax[®] was studied using thermal-gravimetry. The mass loss and the heat exchanges were monitored using a Sensys (Setaram) instrument composed of a thermogravimetric analyzer coupled with a differential scanning calorimeter (TG-DSC). The chemical thermal evolution of Tenax[®] was followed using gas chromatography coupled to mass spectrometry. Analyses were performed on a Trace GC Ultra (ThermoFisher) gas chromatograph equipped with an Optic 3 injector (GL Science, with a maximum operating temperature of 600 °C) and coupled with a quadrupole mass spectrometer DSQ II (ThermoFisher). Electron impact at 70-eV energy was used as the ionization source, and the 45 to 450 *m/z* range was scanned. To characterize the gaseous products released from the sample, GC-MS analyses were completed using two capillary Restek columns: RTX-5Sil-MS (30 m × 0.25 mm × 0.25 μm) and RTX20 (30 m × 0.25 mm × 0.25 μm). The carrier gas was helium (99.9999% purity) set at a 1.0 mL/min flow rate, with a 20 mL/min (RTX-5Sil-MS) or 10 mL/min (RTX20) split flow rate. With the RTX-5Sil-MS, the column temperature started at 35 °C, held for 8 min, and then heated at a 7 °C/min ramp up to 300 °C and held 10 min at this maximum temperature. With the RTX20, the column temperature started at 35 °C, held for 5 min, and then heated at a 10 °C/min ramp up to 300 °C and held 5 min at this maximum temperature.

The samples were prepared for chromatographic analyses using a patented reactor (Buch, Sternberg, & Chazalnoel, 2009) that plays the role of an additional oven located upstream from the Optic 3 injector of the GC-MS (Figure 3).

GC grade derivatization reagents MTBSTFA (99.8%) and DMF (>97%) were purchased from Fluka (France) and Alfa Aesar (France) respectively. Tetrahydrated calcium perchlorate was purchased from Alfa Aesar (France).

The two adsorbents (Tenax® GR and Tenax® TA) were purchased from Interchim (France). Both have a 60–80 mesh size distribution similar to the one used for the SAM's trap. Before analyses, in order to remove any contamination, which could be trapped on the adsorbents, they were cleaned and conditioned. The Tenax® was heated at 280 °C under a 20 ml/min helium flow, either for 24 hr (long conditioning) or 2 hr (short conditioning) to study the effect of conditioning on adsorbent degradation.

Calcium perchlorate ($\text{Ca}(\text{ClO}_4)_2$) was chosen for this study on the basis of its detection in the Rocknest sample (Archer et al., 2014; Glavin et al., 2013; Leshin et al., 2013). As perchlorate salts are highly hygroscopic, they were dehydrated before use in an oven in order to accurately measure the mass of perchlorate handled. Then, the salts of calcium perchlorate were heated at 100 °C to ensure that they were dehydrated. Then, they were put in a hot mortar to keep them dry during crushing. The solidified salts were crushed to form perchlorate shaving. To preserve perchlorate from moisture, they were stored in a desiccator. The determination of percentage of water contained in calcium perchlorate has been done using Karl Fischer Titration (Aquaprocesser radiometer) (Burns & Muraca, 1962). The mean value for the salt we use is around $1\% \pm 0.5\%$

2.2. Thermal Stability of Tenax® TA and GR

To test the thermal stability of Tenax®, 10 mg of Tenax® GR or Tenax® TA was introduced in a glass liner to be preconditioned according to the method described previously. Once this step completed, the Tenax® was heated to a specified temperature ranging from 100 to 600 °C. For each temperature, fresh and clean adsorbent was used. This experiment was repeated 2 times with increasing conditioning duration of 2 and 24 hr. The gaseous products were monitored in real time by GC-MS, using a RTX-20 column.

The physical behavior of Tenax® was also studied with TG-DSC. With this aim, an aluminum crucible containing 10 mg of Tenax® GR or Tenax® TA is flowed with dinitrogen (99.9999% purity) at 50 ml/min. For the original experiment, the initial temperature of Tenax® was set to 280 °C and kept constant for 30 min to clean the adsorbent. After this step was completed, the temperature was increased at a 5 °C/min rate up to 600 °C.

2.3. Study of the Interaction of Tenax® GR With Derivatization Reagents

In order to study the chemical reactivity that can occur between the derivatization reagents and the adsorbents used in SAM, the thermal degradation experiment described above was repeated in the presence MTBSTFA or a mixture of MTBSTFA and DMF. Thus, a 0.5 μl volume of MTBSTFA or MTBSTFA/DMF mixture (4:1) was deposited on 24 hr preconditioned Tenax® GR (long conditioning) in the injector, and the mixture was heated to temperatures ranging from 100 to 600 °C. The gaseous products of reaction were analyzed by GC-MS using the same chromatographic conditions as presented previously.

2.4. Study of the Impact of Calcium Perchlorate on the Adsorbents' Stability

The aim of these experiments was to understand the range of by-products released from the adsorbents (Tenax® GR and TA) when they were exposed to chemically aggressive species such as Cl_2 , HCl, and O_2 released from the perchlorate thermal degradation. In addition, we studied the production of by-products from Tenax® as a function of the amount of perchlorates. The following two different types of experiments were carried out to study this interaction:

1. We placed a long-conditioned sample of adsorbent in direct contact with perchlorate. About 25 mg of Tenax® was placed in the SplitSplex (SSL) GC injector with amounts of perchlorate varying from 3 to 24 mg (~10 to 50wt% of calcium perchlorates; mass fraction is defined as the ratio of the mass of perchlorates to the sum of masses of perchlorates and Tenax®). Then the injector temperature was set to 400 °C (this temperature is above the Tenax® recommended operating temperature and provides a good sample of possible Tenax® by-products) and the gases released from the sample were analyzed by GC-MS.
2. The perchlorate degradation products were sent to the adsorbents from upstream. This experiment allowed a closer approximation of the behavior of the SAM experiment. For these experiments, amounts of $\text{Ca}(\text{ClO}_4)_2$ ranging from ~10 to 50 wt% (from 3 to 24 mg) were placed in the additional oven (Figure 3)

Table 1
List of the Chemical Compounds Detected With GC-MS Analysis During the Thermal Degradation Experiments of Tenax® Alone, and Mixtures of Tenax® With MTBSTFA and MTBSTFA/DMF

No.	Rt (s)	Compound	CAS No.	Short conditioning Tenax® TA	Short conditioning Tenax® GR	Long conditioning Tenax® GR	Long conditioning Tenax® GR + MTBSTFA	Long conditioning Tenax® TA + MTBSTFA/DMF	Source	Compounds detected by SAM
1	199.2	<i>Tert</i> -butyldimethylfluorosilane	NA	N.D.	N.D.	N.D.	350-600	N.D.	MTBSTFA	✓
2	358.8	2,2,2-Trifluoro- <i>N</i> -methylacetamide	815-06-5	N.D.	N.D.	N.D.	100-550	100-600	MTBSTFA	✓
3	446.4	Trimethylsilanol	18173-64-3	N.D.	N.D.	N.D.	100-600	100-600	MTBSTFA	✓
4	285.6	Benzene	71-43-2	400-600	400-600	500-600	500-600	600	TENAX	✓
5	446.4	<i>Tert</i> -butyldimethylsilanol (MSW)	18173-64-3	N.D.	N.D.	N.D.	100-600	100-600	MTBSTFA - H ₂ O	✓
6	455.4	Toluene	108-88-3	500-600	400-600	550-600	200-600	500-600	TENAX	✓
7	575.4	<i>N,N</i> -dimethylformamide (DMF)	68-12-2	N.D.	N.D.	N.D.	N.D.	100-600	DMF	N.D.
8	574.2	Ethylbenzene	100-41-4	550-600	450-600	550-600	550-600	550-600	TENAX	✓
9	600	Phenylethyne	536-74-3	450-600	450-600	N.D.	500-600	550-600	TENAX	✓
10	616.8	Styrene	100-42-5	400-600	400-600	550-600	550-600	550-600	TENAX	✓
11	675.6	2,2,2-Trifluoro- <i>N</i> -methyl- <i>N</i> -(trimethylsilyl)acetamide	24589-78-4	N.D.	N.D.	N.D.	100-600	100-300	MTBSTFA	✓
12	720.6	Benzene, 1-ethenyl-2-methyl or	611-15-4	400-600	400-600	N.D.	450-600	N.D.	TENAX	N.D.
13	723.6	Benzene, 2-propenyl or <i>o</i> -methylstyrene, or <i>p</i> -methylstyrene, or <i>m</i> -methylstyrene	300-57-2 98-83-9 622-97-9	400-600	400-600	600	400-600	550-600	TENAX	✓
14	734.4	<i>N,N</i> -diamylmethylamine	76257-73-3	N.D.	N.D.	N.D.	100-600	100-250	DMF	N.D.
15	777.6	Phenol	108-95-2	400-600	400-600	600	400-600	550-600	TENAX	✓
16	801	1,3-Ditert-butyl-1,1,3,3-tetramethyldisiloxane (BSW)	67875-55-2	N.D.	N.D.	N.D.	100-600	100-600	MTBSTFA - H ₂ O	✓
17	808.8	Benzene, 1-propenyl or benzene, 1-ethenyl-3-methyl	673-32-5 766-82-5	N.D.	450-600	N.D.	450-600	550-600	TENAX/MD	N.D.
18	847.8	Cresol	1319-77-3	N.D.	N.D.	N.D.	500-600	600	TENAX/MD	N.D.
19	864	Acetophenone	98-86-2	500-600	400-600	N.D.	300-600	550-600	TENAX/MD	N.D.
20	930	Benzene,1-methyl-4-(2-propenyl)-	3333-13-9	N.D.	N.D.	N.D.	550-600	600	TENAX/MD	N.D.
21	936	Tris-(trimethylsilyl)borate	4325-85-3	N.D.	N.D.	N.D.	100-600	100-250	MTBSTFA	✓
22	951.6	Benzoic acid	65-85-0	400-450	N.D.	N.D.	N.D.	N.D.	TENAX	N.D.
23	993	Naphthalene	2471-84-3	400-600	400-600	500-600	350-600	500-600	TENAX	✓
24	1,038	3-Phenyl-3-butene-2-one	32123-84-5	N.D.	N.D.	N.D.	550-600	N.D.	TENAX/M	N.D.
25	1,114.2	Bis-(<i>tert</i> -butyldimethylsilyl)carbonate	NA	N.D.	N.D.	N.D.	100-600	100-400	MTBSTFA	N.D.
26	1,125.6	Diphenyldifluorosilane	312-40-3	N.D.	N.D.	N.D.	350-600	N.D.	MTBSTFA	N.D.
27	1,158	Biphenyl	92-52-4	400-600	400-600	450-600	300-600	500-600	TENAX	✓
		Benzoic acid, TBDMS	75732-41-1	N.D.	N.D.	N.D.	250-600	N.D.	TENAX/M deriv.	✓

Table 1 (continued)

No.	Rt (s)	Compound	CAS No.	Short conditioning Tenax® TA	Short conditioning Tenax® GR	Long conditioning Tenax® GR	Long conditioning Tenax® GR + MTBSTFA	Long conditioning Tenax® TA + MTBSTFA/DMF	Source	Compounds detected by SAM
28	1,149.6	1H-indene-1,3(2H)-dione	606-23-5	450-500	N.D.	N.D.	N.D.	N.D.	N.D.	N.D.
29	1,164.6	Diphenylmethane or 2-Methylbiphenyl	101-81-5	400-600	400-600	450-600	400-600	550-600	TENAX	N.D.
	1,209.6		643-58-3							
30	1,227	Stilbene	588-59-0	400-500	N.D.	N.D.	N.D.	N.D.	N.D.	N.D.
31	1,254.6	<i>o</i> -Hydroxy-biphenyl or	90-43-7	400-550	400-600	450-600	150-600	500-600	TENAX	N.D.
	1,399.8	<i>p</i> -Hydroxybiphenyl or	92-69-3							
		<i>m</i> -Hydroxybiphenyl or	580-51-8	450-550	400-600	N.D.	300-600	N.D.	TENAX/M	N.D.
32	1,291.8	Fluorene	86-73-7	400-550	N.D.	500-600	500-600	N.D.	TENAX/M	N.D.
33	1,288.2	<i>p</i> -Benzylphenol	39579-09-4	450-600	N.D.	N.D.	500-600	N.D.	TENAX/M	N.D.
34	1,338	4-Phenyl-4-cyclopentene-1,3-dione	51306-96-8	450-600	N.D.	N.D.	500-600	N.D.	TENAX/M	N.D.
35	1,453.2	9H-fluorene, 9-methylene	85-01-8	450-600	N.D.	N.D.	500-600	N.D.	TENAX/M	N.D.
36	1,483.2	1-Benzyl-naphthalene	611-45-0	450-550	N.D.	N.D.	500-600	N.D.	TENAX/M	N.D.
37	1,509	[1,1'-biphenyl]-2,5-diol	1079-21-6	400-600	400-600	N.D.	350-600	500-600	TENAX/ MD	N.D.
		[1,1'-biphenyl]-4,4'-diol	92-88-6	450-500	400-600	N.D.	300-600	500-600	TENAX/ MD	N.D.
38	1,561.2	2-Phenyl-naphthalene	35465-71-5	400-550	400-600	500-600	250-600	500-600	TENAX/ MD	N.D.
39	1,682.4	Terphenyl	26140-60-3	400-600	400-600	400-600	250-600	500-600	TENAX/ MD	N.D.
40	1,723.8	<i>m</i> -Terphenyl-2'-ol or <i>m</i> -terphenyl-4'-ol	2432-11-3	400-600	400-600	400-600	250-600	500-600	TENAX	ND
	1,794		6093-03-4							
	1,874.4									
41	1,780.8	Indeno[2,1b]oxine, 2-phenyl or	10435-	400-600	400-600	550-600	350-600	500-600	TENAX	N.D.
	1,797.6	Dibenzofuran, 4-phenyl or	67-3							
	1,818.6	dibenzofuran, 1-phenyl	74104-10-							
			2 6331-							
			7 69-1							
42	1,807.8	<i>m</i> -Terphenyl, 5' phenyl or	612-71-5	N.D.	N.D.	N.D.	600	500-600	TENAX/ MD	N.D.
	2,103	Quaterphenyl	29036-02-0							
	2,134.2									
43	1,861.8	2,5-Cyclohexadiene-1,4-dione, 2,5-diphenyl-	844-51-9	N.D.	N.D.	N.D.	600	500-600	TENAX/ MD	N.D.
44	1,965.6	2,4,6-Triphenylphenol	3140-01-0	N.D.	N.D.	N.D.	600	N.D.	TENAX/M	N.D.
	2,001.6									
	2,019.6									

Note. They are presented with their retention times, their CAS numbers, and the temperatures at which they are released. A specific column corresponds to the compounds detected by SAM. Abbreviations: DMF: dimethylformamide; GC-MS: gas chromatograph mass spectrometer; MTBSTFA - H₂O: derivatization products of water by MTBSTFA (MSW: monosilylated water/BSW: bisilylated water); N.D.: not detected; SAM: Sample Analysis at Mars; TENAX: Tenax® degradation by-products observed with or without addition of the derivatized products (MTBSTFA or MTBSTFA/DMF mixture); TENAX/M: non-derivatized molecules formed from Tenax® only in the presence of MTBSTFA (certainly due to MTBSTFA by-product i.e. HF); TENAX/M deriv.: the TBDMS-benzoic acid is the result of the derivatization by MTBSTFA of Tenax® degradation product i.e. benzoic acid; TENAX/MD: non-derivatized Tenax® products generated only after the addition of MTBSTFA or of MTBSTFA/DMF mixture.

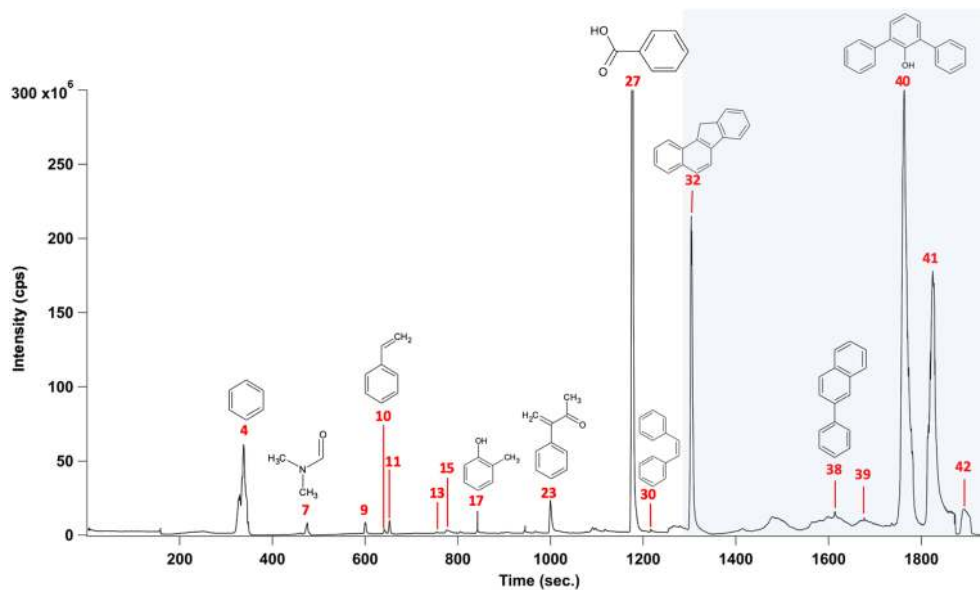


Figure 4. Chromatogram obtained on a RTX20 (Restek) column when analyzing the compounds released by Tenax[®] TA heated up to 600 °C (the numbers correspond to those presented in Table 1). The shaded part corresponds to all the compounds unable to be seen by Sample Analysis at Mars due to their high retention times. Temperature program: 35 °C hold for 5 min then 10 °C/min up to 300 °C then isotherm at 300 °C for 5 min.

and heated to 400 °C (± 10 °C). Gaseous degradation products were sent to the optic 3 injector, which contains Tenax[®] GR cooled to 0 °C (using CO₂ cooling) for 5 min. Desorption occurred at 300 or 400 °C. The approximate maximal temperature reached by Tenax[®] in SAM trap is set between those two temperatures (Glavin et al., 2013; Leshin et al., 2013).

Tenax[®] GR adsorbent is contained in the HC traps of SAM placed upstream from the IT. As a result, these traps are the first exposed to derivatization solvent or perchlorates by-products, and thus the most likely impacted. For this reason, we prioritized the use of Tenax[®] GR for these experiments with pure MTBSTFA, mixed MTBSTFA/DMF, and finally with perchlorates.

3. Results and Discussions

3.1. Thermal Degradation of Tenax[®] GR and TA

3.1.1. Thermal Degradation Products

The effect of temperature on Tenax[®] TA and Tenax[®] GR degradation was investigated up to 600 °C, which is higher than the maximum temperature used for SAM (300 °C) for trap heating. The molecules detected are presented in Table 1. A typical chromatogram obtained from the heating of the Tenax[®] TA to 600 °C is displayed in Figure 4.

In Table 1, we observe that the short conditioning Tenax[®] TA and the short conditioning Tenax[®] GR starts to release volatile products from 400 °C. Twenty-five and 19 organic molecules were detected, respectively, a majority of them containing aromatic rings. The size of these compounds ranged from C₆ to C₂₄ (Table 1). We separated them into four groups such as phenyl (which contains one aromatic cycle of 6 carbons, e.g., benzene and acetophenone), biphenyl (e.g., biphenyl and hydroxybiphenyl), terphenyl (e.g., terphenyl) derivatives, and other molecules that are produced either by cyclization or recombination including naphthalene, benzofurane, stilbene, and fluorene derivatives.

3.1.2. Degradation Mechanisms of Tenax[®]

To explain the thermal decomposition of the Tenax[®] and the formation of the detected by-product (Table 1), we follow a general mechanism of thermal decomposition of polymers (Witkowski et al., 2016). The alteration of the polymer is initiated by (1) the main chain reaction, a random-chain scission (the decomposition reaction produces monomers or oligomers including ten monomers units maximum) and the cross-linking between unsaturated site, or (2) the side chain reaction, a side chain elimination (the decomposition takes place at the adjacent groups) and side chain cyclization. Then, the decomposition of the polymer

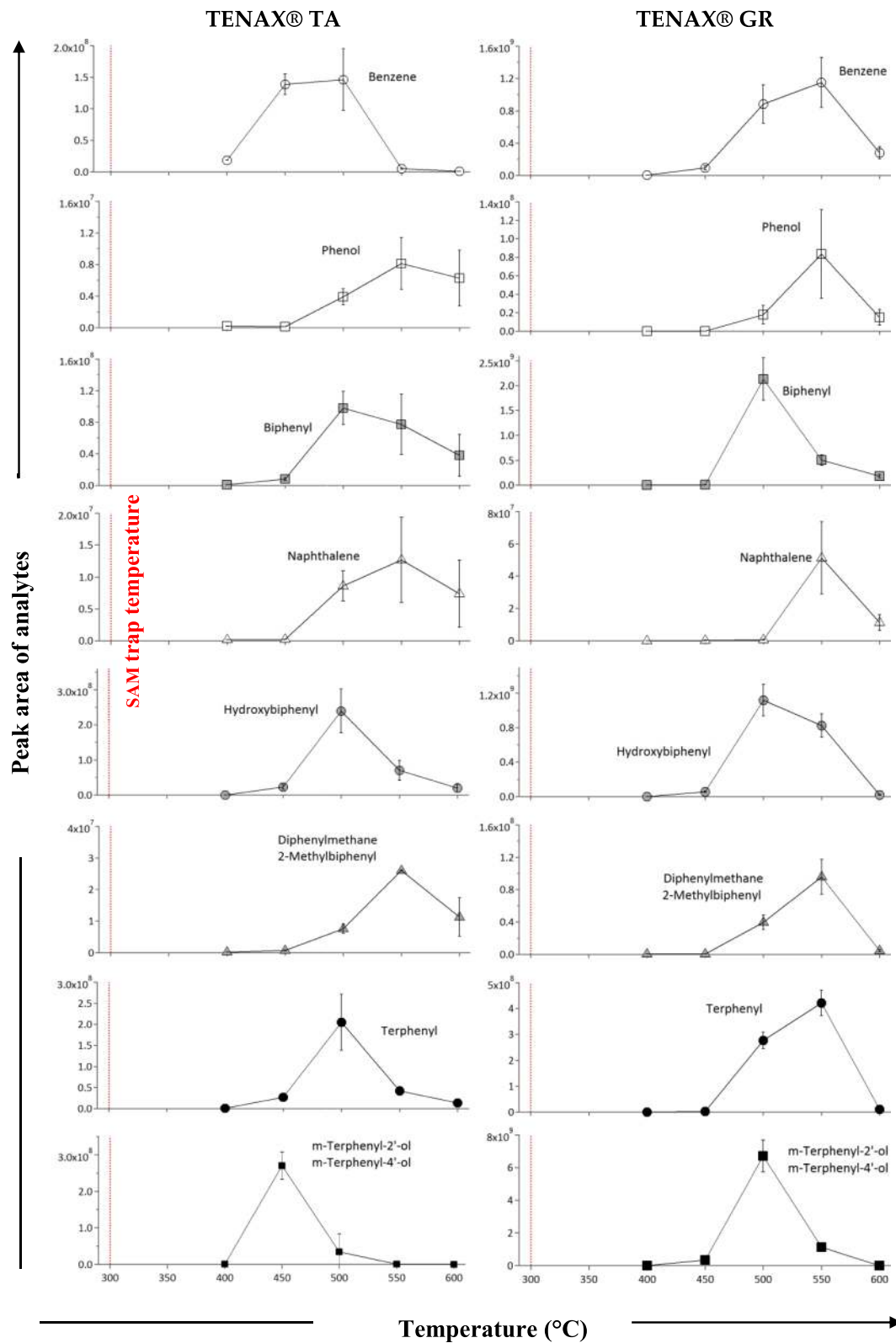


Figure 5. Evolution of the quantity of compounds released from Tenax® GR and TA versus the temperature for the benzene (m/z 78), phenol (m/z 94), naphthalene (m/z 128), hydroxybiphenyl (m/z 170), biphenyl (m/z 154), diphenylmethane-2-methylbiphenyl (m/z 168), terphenyl (m/z 230), and *m*-terphenyl-2'-ol/*m*-terphenyl-4'-ol (m/z 246). Maximum temperature of the Sample Analysis at Mars trap is 300 °C (red line).

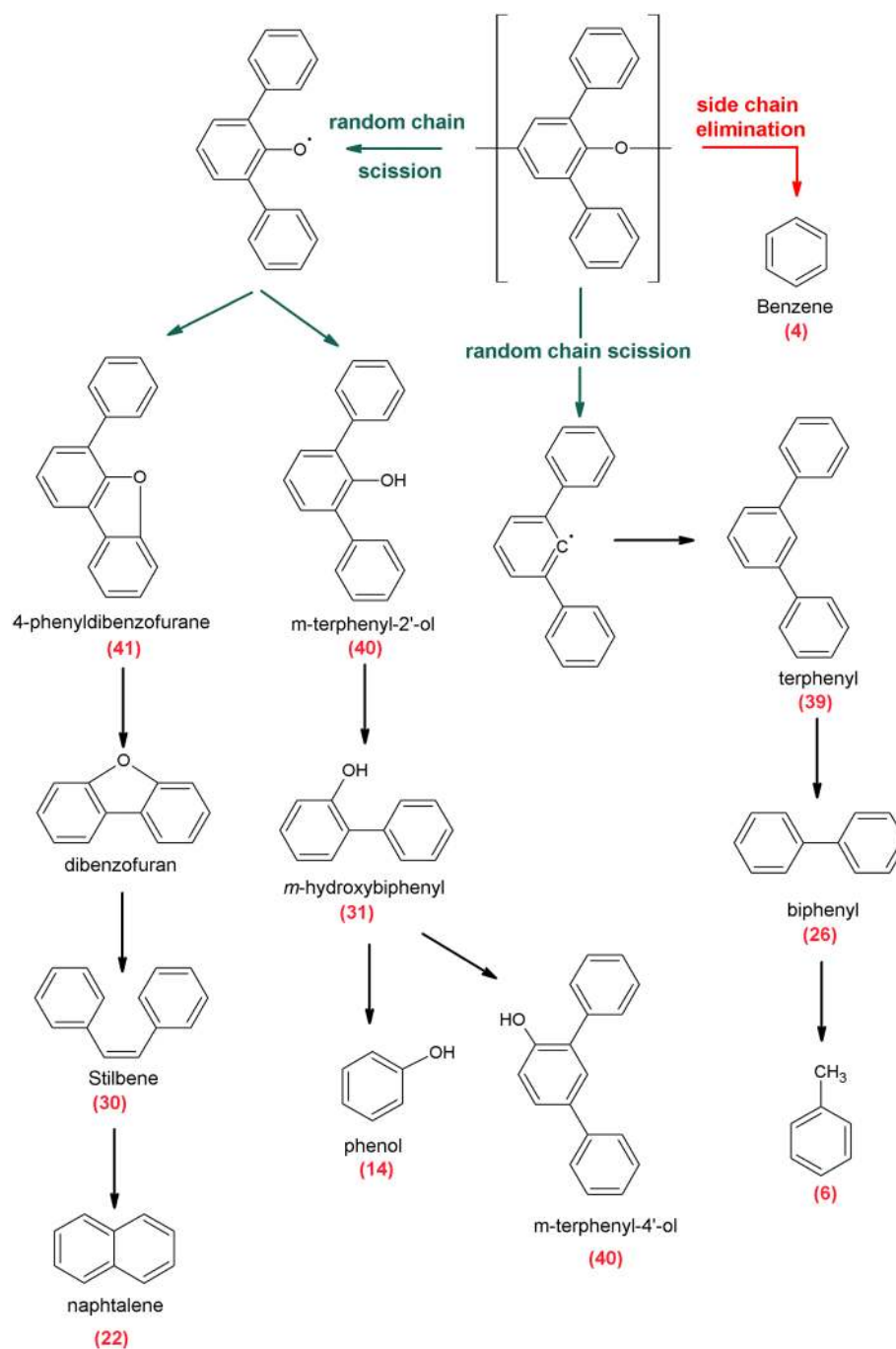


Figure 6. Mechanisms of thermal degradation of the Tenax[®] by side chain elimination and random chain scission. The pathway of formation for Tenax[®] certain artifacts is listed in Table 1. The numbers in brackets correspond to the number of compounds listed in Table 1.

propagates through hydrogen atom transfer (intramolecular and intermolecular transfer) and decomposition of the polymer (depolymerization). Finally, a termination neutralizes the propagation of the decomposition of the polymer by the assembly of two polymer chain radicals (recombination), by the transfer of hydrogen radicals from another polymer chain (disproportionation) or from an unimolecular termination.

To elucidate the mechanism of thermal degradation of Tenax[®] GR and Tenax[®] TA and the formation of the species released during degradation, the abundances of their major thermal degradation products are plotted as a function of temperature (Figure 5).

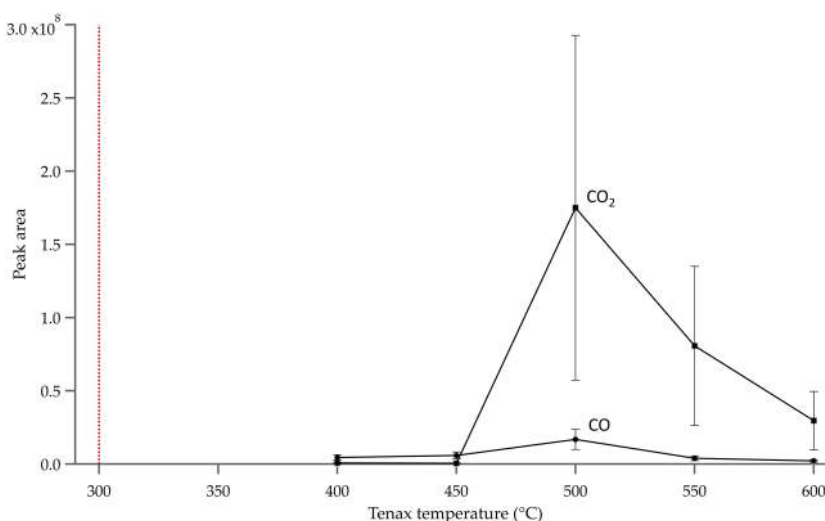


Figure 7. Evolution with temperature of the amount of Tenax[®] GR and Tenax[®] TA major thermal degradation products, that is, benzene (m/z 78), phenol (m/z 94), naphthalene (m/z 128), hydroxybiphenyl (m/z 170), biphenyl (m/z 154), diphenylmethane/2-methylbiphenyl (m/z 168), terphenyl (m/z 230), and *m*-terphenyl-2'-ol/*m*-terphenyl-4'-ol (m/z 246).

The products of thermal degradation of the Tenax[®] GR adsorbents begin to be released at 400 °C. The emission of *m*-terphenyl-2'-ol/*m*-terphenyl-4'-ol (isomers), biphenyl, and hydroxybiphenyl reached their maximum intensity at 500 °C for Tenax[®] GR. At this same temperature, other molecules, namely, benzene, diphenylmethane/2-methylbiphenyl (isomers), terphenyl, and phenol also started to evolve. Nevertheless, their maximum rate of production was observed around 550 °C. With Tenax[®] GR, the naphthalene peak emerged only at 550 °C.

With regard to Tenax[®] TA, the release of polymer thermal degradation products started at the same temperature as Tenax[®] GR, 400 °C. However, the formation of *m*-terphenyl-2'-ol/*m*-terphenyl-4'-ol and benzene reached their maximum of intensity at 450 °C. Hydroxybiphenyl, terphenyl, biphenyl, and benzene were produced at 500 °C as well as diphenylmethane/2-methylbiphenyl, naphthalene, and phenol, which peaked at 550 °C. For all compounds and both Tenax[®] TA and GR, the abundance of thermal degradation products drastically decreased from 600 °C.

These results appear to indicate that the thermal decomposition of Tenax[®] (Figure 6) occurred through random chain scission first, leading to the formation of *m*-terphenyl-2'-ol/*m*-terphenyl-4'-ol when the adsorbent degradation began (Figure 5; Tenax[®] TA at 450 °C and Tenax[®] GR at 500 °C). Then, at higher temperatures (around 450 and 500 °C), smaller molecules including terphenyl, hydroxybiphenyl, and biphenyl came out either directly from PPPO polymer by random chain scission or from of Tenax[®] by-products by thermal degradation. The compounds observed could have been the result of the degradation of larger molecules or the



Figure 8. Picture of the dark residues deposited in the gas chromatograph-mass spectrometer liner after the exposure to 600 °C of 50 mg of Tenax[®] GR contained in the liner.

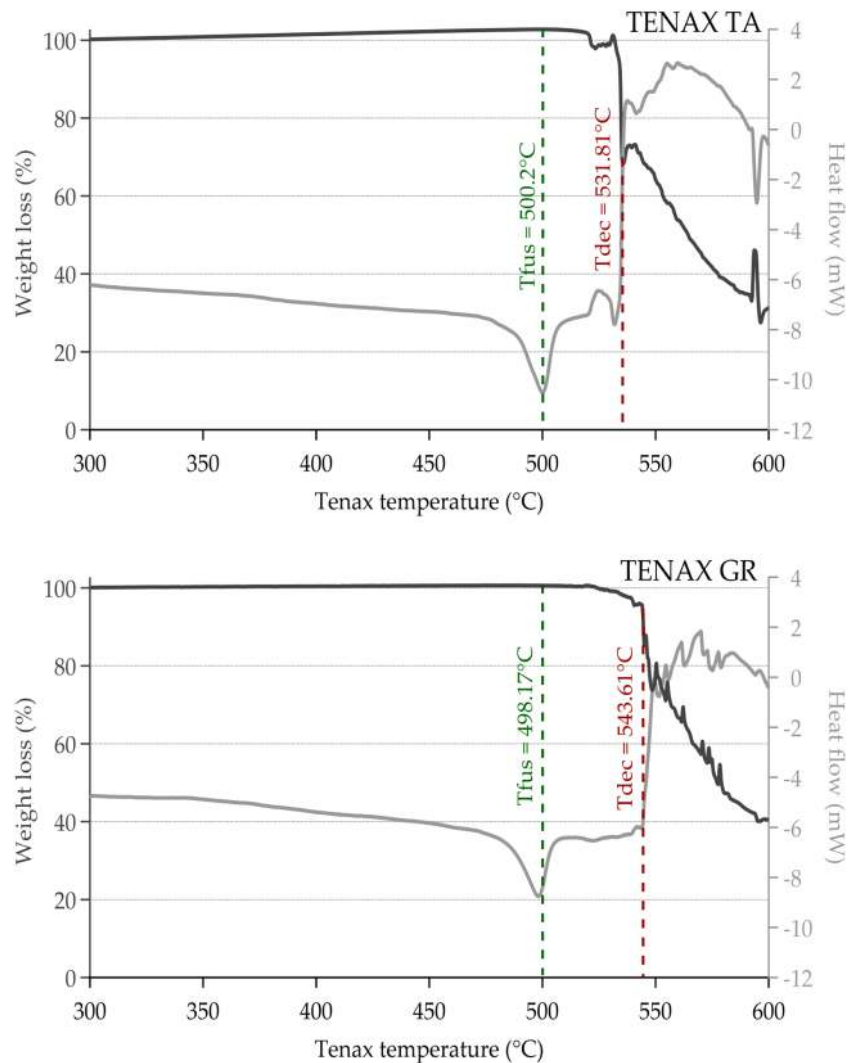


Figure 9. Weight loss (dark grey) and heat flow (light grey) of Tenax® GR and Tenax® TA (10 mg each) measured between 300 and 600 °C. (T_{fus} and T_{deg} are respectively defined as the temperature of fusion and the temperature of the onset of degradation).

recombination of smaller compounds. For instance, biphenyl might have been formed either from the thermal decomposition of terphenyl or from the recombination of phenyl fragments (Masonjones et al., 1996; Silverman et al., 2007). Diphenylmethane, 2-methylbiphenyl and naphthalene could have been caused respectively by recombination of phenyl fragments or cyclization of phenyl derivatives (Bittner & Howard, 1981; Colket & Seery, 1994; Frenklach et al., 1985). The fact that they were mostly formed at high temperature (550 °C) is due to the production of phenyl derivatives at this temperature.

Benzene, however, is an interesting case. This molecule can be formed by many pathways specifically by the secondary decomposition of larger Tenax® degradation products (e.g., terphenyl and biphenyl; Figure 6) or directly from the polymer by the side chain elimination process (Witkowski et al., 2016). This latter way of production directly from the Tenax® explains why the benzene is produced at lower temperatures than the other by-products (400 °C from Tenax® TA).

Finally, at 600 °C, the amount of carbon dioxide and carbon monoxide also decreased (Figure 7); thus, it follows that the amount of Tenax® by-products decreased drastically (Tenax® by-products are not transformed into carbon oxides). Still, the observation of a dark solid residue for both Tenax® GR deposited inside the

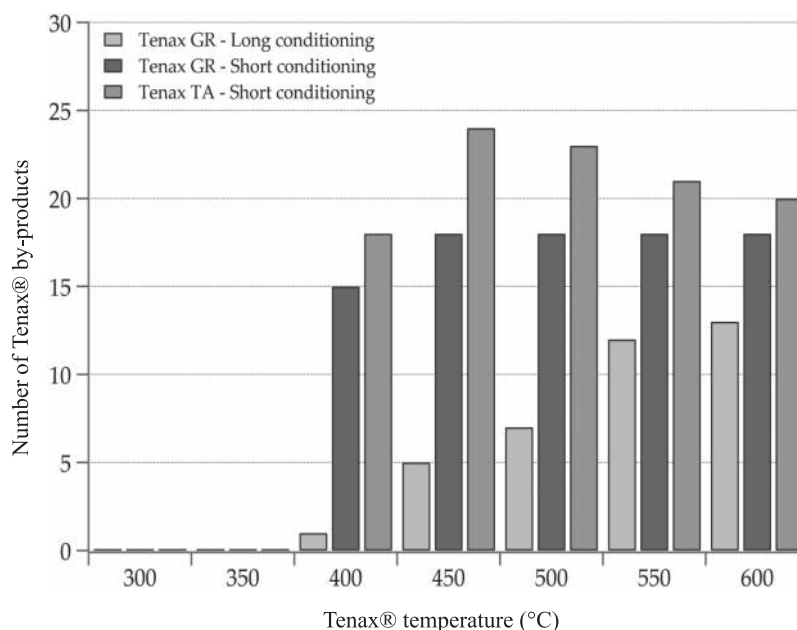


Figure 10. Number of molecules (above the three times noise level) produced after short conditioning Tenax® TA (medium grey), short conditioning Tenax® GR (dark grey), and long conditioning Tenax® GR (light grey) as a function of temperature (400 to 600 °C).

liner seems to indicate the formation of condensate organic compounds in the gaseous phase that are refractory to GC-MS analysis (Figure 8). Indeed, it had been observed that these residues are not degraded at high temperatures (up to ~600 °C) in inert gas conditions; they can only be removed by a combustion processes (e.g., clean up on ambient air [with O₂] at 500 °C). These condensate OMs happened to be soot (i.e., products of the gas-phase incomplete combustion of organics) produced in the gaseous phase and sensitive to the presence of oxygen (Hamins, 1993; Moldoveanu & David, 2002; Omidvarborna et al., 2015; Wampler, 2006).

3.1.3. Thermal Properties of Tenax®

Thermal analysis devices included a DSC that measures the energy exchange of the sample (heat flow curve) as well as a thermogravimetric analysis device (TGA) used to detect mass variation of samples at the mg-scale (weight loss, Figure 9).

Below 500 °C, Tenax® TA and GR were stable (i.e., no mass variation and no heat flow peak observed). Above this temperature, we observed two major phenomena: an endothermic peak around 500 °C and a rapid decrease of sample mass associated with an increase of the heat flow commencing above 530 °C. The exothermic peak observed at the sample temperature for the two adsorbents (i.e., at 498.17 °C for Tenax® GR and 500.02 °C for Tenax® TA) corresponded to the melting temperature, estimated to be around 500 °C based on previous papers (Gaur & Wunderlich, 1981; Weyland et al., 1970; Wrasidlo, 1971). With regard to the decrease of the mass of samples above 530 °C, we conclude that it resulted from the degradation of the polymer. Thus, the difference between the two adsorbents was visible in terms of temperature of degradation, with the degradation of Tenax® TA starting at a slightly lower temperature (531.87 ± 0.20 °C) than Tenax® GR (543.61 ± 0.20 °C). At 600 °C, Tenax® GR and Tenax® had respectively lost 60% and 69% of their initial sample mass. We also observed that the physical structure of Tenax® was altered. After heating, the adsorbent formed a black solid aggregate.

The variation observed between Tenax® TA and GR can be explained by the composition and the structure of the adsorbents. The Tenax® GR, a mixture of poly(2,6-diphenylphenylene oxide (PPPO) polymer with graphitic carbon, contains a larger additional source of organic carbon than Tenax® TA, which is completely composed of PPPO. In addition, the specific surface area of Tenax® GR and Tenax® TA are 24 and 35 m²/g, respectively (Lee et al., 2006). As a result, Tenax® TA is more vulnerable to the temperature because a larger surface is exposed to heat. We note that the variation between TGA-DSC and GC-MS analyses can be

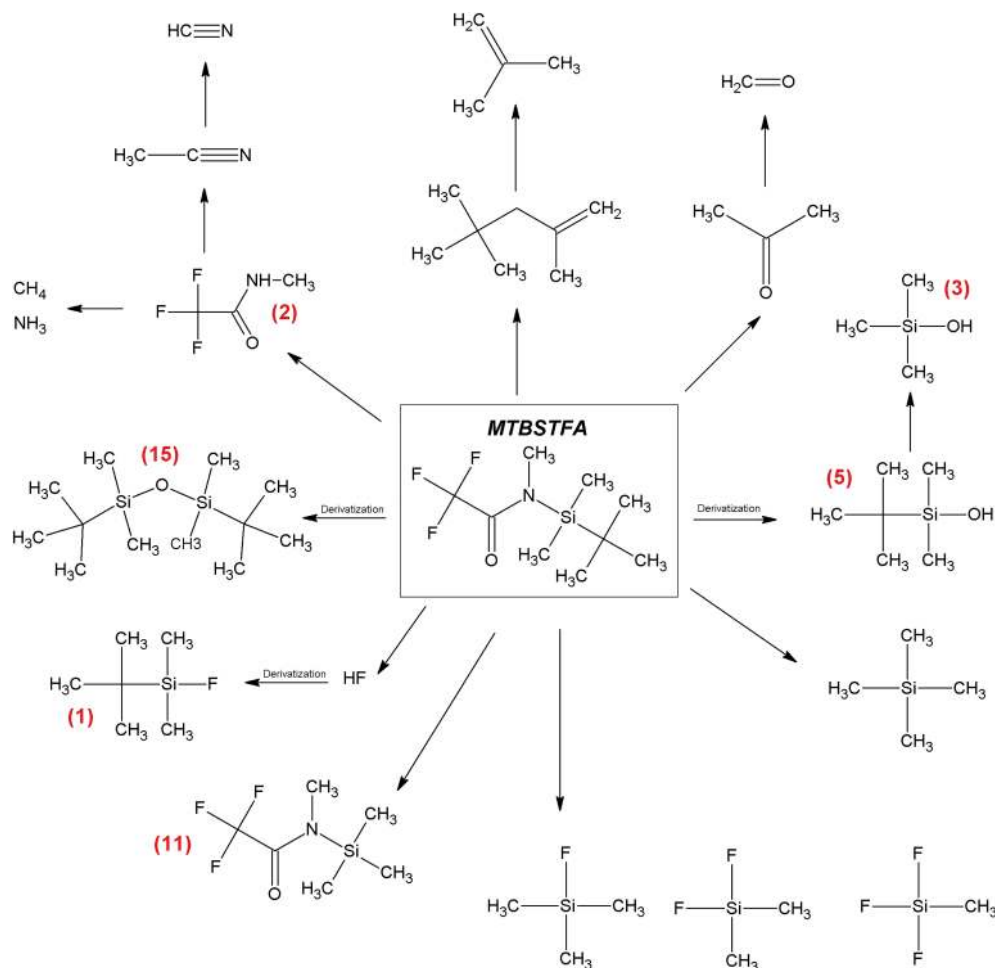


Figure 11. By-products of the *N*-tert-butyltrimethylsilyl-*N*-methyltrifluoroacetamide (MTBSTFA) detected in this study and by Sample Analysis at Mars. Products with a number in brackets correspond to the number of compounds listed in Table 1.

explained by the heating rate used for both analyses (5 °C/min and ~20 °C/s, respectively). As the heating rate decreases, it has been shown that decomposition initiation begins at lower temperatures (Sichina, 2011).

One minor phenomenon is noticeable in Figure 9: above the melting temperature, mass loss fluctuation is more important for Tenax® TA and GR. For example, for Tenax® GR, we observed a sudden and temporary increase of mass around 590 °C. Combined with the observation of a dark solid residue in the TGA-DSC sample holder used to suspend the crucible, we conclude that these variations were caused by the condensation and volatilization of soot.

3.1.4. Effect of Conditioning

As shown in Figure 10, after a long conditioning (24 hr), Tenax® GR released fewer by-products upon heating, qualitatively speaking, than after a short conditioning procedure (2 hr). In addition, the quantitative abundance of these by-products was also reduced, and degradation products were formed at higher temperatures after 24 hr of conditioning (with the exception of *m*-terphenyl-2'-ol/*m*-terphenyl-4'-ol, which started to be released at the same temperature (400 °C) regardless of the conditioning duration). In addition, when we compared Tenax® GR conditioned for 2 hr with the Tenax® TA conditioned for 2 hr, we observed that fewer compounds were formed from Tenax® GR regardless of the Tenax® temperature (400 to 600 °C; Figure 10). To summarize, it seems that the decrease of the conditioning duration accentuates the formation of degraded species, and Tenax® TA is more sensitive to thermal degradation than Tenax® GR. This finding is consistent with the results of the TG-DSC analysis described above.

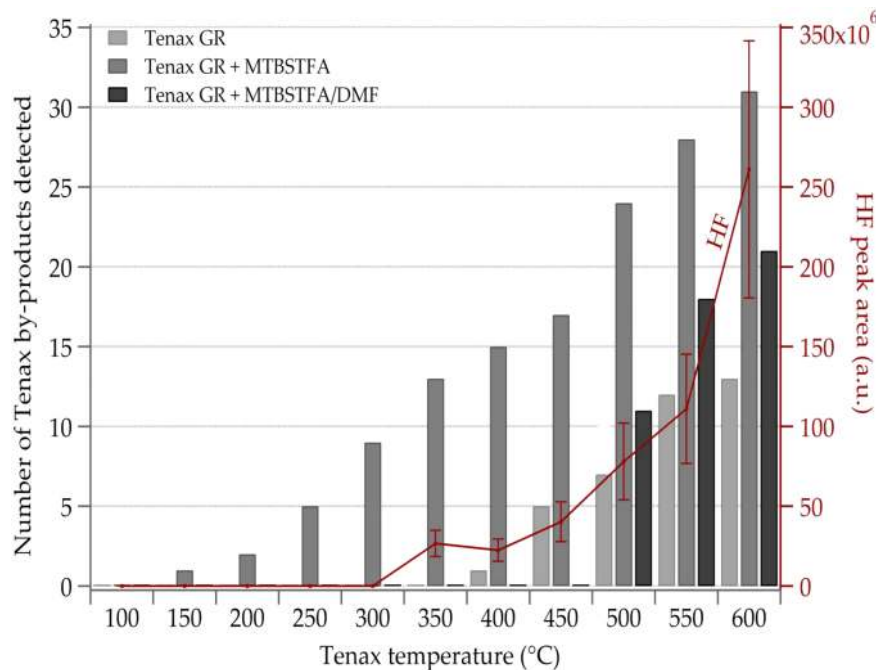


Figure 12. Number of detected compounds (above the three times noise level) released by long conditioning Tenax[®] GR (light grey), long conditioning Tenax[®] GR mixed with 0.5 μ l of *N*-tert-butyltrimethylsilyl-*N*-methyltrifluoroacetamide (MTBSTFA; medium grey), and long conditioning Tenax[®] GR with 0.5 μ l of mixture of MTBSTFA/dimethylformamide (DMF; 4:1; dark grey) as function of temperature (100–600 °C) and the evolution of the quantity of hydrofluoric (HF) (corresponding to the sum of the amount of fluorinated compounds formed from HF, that is, TDBMS-F and diphenyldifluorosilane) detected during Tenax[®] GR and MTBSTFA experiments.

In general, the main by-products observed from Tenax[®] were due to the release of residues (impurities introduced in the manufacturing process) from the fabrication of Tenax[®] and also by the degradation of the adsorbent because of the effect of oxidants (e.g., NO_x or O₃). Some other by-products are also due to the emission of the previous analytes trapped in the Tenax[®] (Cao & Hewitt, 1994; Lee et al., 2006). The difference between Tenax[®] GR with short or long conditioning is thought to be due to the better efficiency of the elimination of Tenax[®] fabrication residues, of Tenax[®] degradation products at low temperature (<280 °C) and the adsorbed compounds during the storage.

During experiments performed with the SAM instrument on Mars, the maximum temperatures of the injection traps were set at <300 °C, temperatures which are normally below the temperature of degradation of Tenax[®]. However, aromatic chemical species were detected by SAM GC-MS in various samples, including a large number of molecules likely to be formed from Tenax[®], such as cyclopentene, cyclopentadiene, benzene, toluene, chlorobenzene, ethylbenzene, xylene, phenylethyne, TBDMS-phenol (from Tenax[®] and MTBSTFA reaction), styrene, naphthalene, and biphenyl (Ming et al., 2014).

To investigate this further, we also considered factors that may enhance the degradation of Tenax[®]. First, we analyzed the effect of the derivatization reagent MTBSTFA and solvent DMF. These two reagents are contained in SAM derivatization cups and are used for wet chemistry experiments. A leak of MTBSTFA/DMF has been observed in SAM, which could impact the by-products release of Tenax[®] (Glavin et al., 2013). Second, we considered the presence of oxidants. It has been demonstrated that the Martian soil contains perchlorate salts can be decomposed into oxygen, hydrochloric acid, and chlorine (Glavin et al., 2013; Migdał-Mikuli & Hetmańczyk, 2008), which also may have an impact on the stability of Tenax[®] when the molecules come in contact with the adsorbent (Klenø et al., 2002; Lee et al., 2006). While studies have been conducted to define the backgrounds that may be induced by exposure to oxidizing medium on Tenax[®], Tenax[®] has been largely used to analyze atmospheric composition. The experiments reported in the literature thus far focus on the impact of gases and molecules present in the atmosphere, including ozone O₃, oxides of nitrogen NO_x, and organic molecules that lead to the production of artifacts. For instance, Jae Hwan Lee (Lee et al., 2006) examined the influence of ozone in contact with the polymer Tenax[®], demonstrating the production

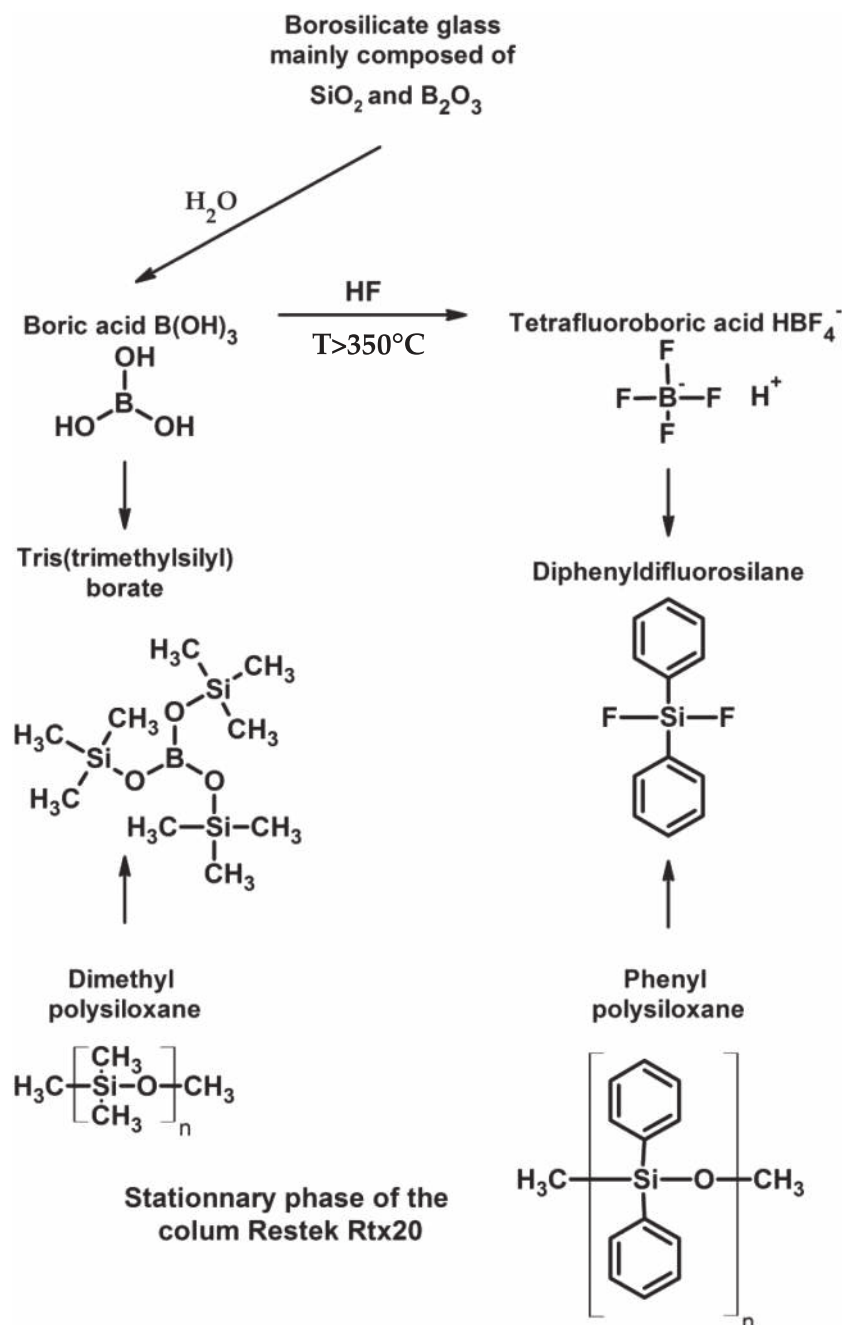


Figure 13. Possible mechanism of formation of Tri (trimethylsilyl)borate and diphenyldifluorosilane from column stationary phase, borosilicate glass, and *N*-tert-butyltrimethylsilyl-*N*-methyltrifluoroacetamide degradation products.

of some organic compounds similar to those found during our experiments, including phenol and acetophenone (Klenø et al., 2002; Lee et al., 2006). Finally, the impact of perchlorate on Tenax® was analyzed to determine if this polymer adsorbent could be a source of chlorinated aromatic compounds like the chlorobenzene and dichlorobenzene that have been detected by SAM.

3.2. Impact of the Derivatization Reagent MTBSTFA and the Solvent DMF on Tenax® Degradation at Various Temperatures

As a very reactive reagent, MTBSTFA is able to damage the stationary phase of chromatographic columns by interacting with the silanol groups and increasing column bleed. As the same reactivity is expected when

Table 2

List of the Compounds Detected With GC-MS Analysis When Heating Mixtures of Tenax® Adsorbents and Perchlorates

No.	t_R (s)	Compound	CAS No.	Base peak m/z	Long conditioning Tenax® GR	Long conditioning Tenax® TA	Compounds detected by SAM
1	157.8	Cyclopentene	142-29-0	67	N.D.	✓	N.D.
2	243.6	1,3-Cyclopentadiene	542-92-7	66	✓	N.D.	N.D.
3	297	Benzene	71-43-2	78	✓	✓	✓
4	426.6	Toluene	108-88-3	91	✓	✓	✓
5	442.8	1,2,3-Norcaratriene	4646-69-9	90	✓	N.D.	N.D.
6	603.6	Benzene, chloro	108-90-7	112	✓	✓	✓
7	637.2	Benzene, ethyl	100-41-4	91	✓	N.D.	✓
8	657	Xylene	108-38-3	91	✓	N.D.	✓
			95-47-6				
			106-42-3				
9	676.2	Phenylethyne	536-74-3	102	✓	✓	✓
10	703.8	Styrene	100-42-5	104	✓	✓	✓
11	805.8	Benzene, 1-ethenyl-2-methyl or Benzene, 2-propenyl or Styrene, α -methyl or	611-15-4 300-57-2 98-83-9	117	✓	✓	N.D.
12	840	Benzaldehyde	100-52-7	77	✓	✓	N.D.
13	885	Phenol, 2-chloro or Phenol, 3-chloro	95-57-8 108-43-0	128	✓	N.D.	N.D.
14	892.8	Benzofuran	271-89-6	118	✓	✓	N.D.
15	902.4	Phenol	108-95-2	94	✓	✓	✓
16	923.4	Benzene, 1,2-dichloro or Benzene, 1,3-dichloro or Benzene, 1,4-dichloro	95-50-1 541-73-1 106-46-7	146	✓	✓	✓
17	945.6 970.2 976.8 999	Benzene, 1-ethynyl-3-methyl or Benzene, 1-ethynyl-4-methyl or Benzene, 1-propynyl- or Benzene, 2-propynyl-	766-82-5 766-97-2 673-32-5 10147-11-2	115	✓	N.D.	N.D.
18	964.8	2-Chloroethynylbenzene	1483-82-5	136	✓	✓	N.D.
19	1,017	Benzoyl chloride	98-88-4	105	✓	✓	N.D.
20	997.2 1,031.4	Phenol, 2-methyl or Phenol, 3-methyl or Phenol, 4-methyl	95-48-7 108-39-4 106-44-5	108	✓	N.D.	N.D.
21	1,041.6 1,159.8	1,4-Diethynylbenzene	935-14-8	126	✓	N.D.	N.D.
22	1,067.4	2-Methylbenzofuran or 3-Methylbenzofuran or 7-Methylbenzofuran	4265-25-2 21535-97-7 17059-52-8	131	✓	N.D.	N.D.
23	1,083 1,092 1,103.4	Benzaldehyde, 2-chloro or Benzaldehyde, 3-chloro or Benzaldehyde, 4-chloro	89-98-5 587-04-2 104-88-1	131	✓	N.D.	N.D.
24	1,099.8 1,165.2 1,207.2	Benzene, 1,2,3-trichloro or Benzene, 1,2,4-trichloro or Benzene, 1,3,5-trichloro	87-61-6 120-82-1 108-70-3	182 180	✓	✓	N.D.
25	1,117.8	Benzofuran, 5-chloro- or Benzofuran, 7-chloro-	23145-05-3 24410-55-7	152	✓	✓	N.D.
26	1,138.2	Naphtalène	91-20-3	128	✓	✓	✓
27	1,153.2 1,462.8	Phenol, 2,4-dichloro or Phenol, 2,5-dichloro or Phenol, 2,6-dichloro or Phenol, 3,4-dichloro or	120-83-2 583-78-8 87-65-0 95-77-2	162	✓	N.D.	N.D.

Table 2 (continued)

No.	t_R (s)	Compound	CAS No.	Base peak m/z	Long conditioning Tenax® GR	Long conditioning Tenax® TA	Compounds detected by SAM
28	1,176	Phenol, 3,5-dichloro 2,2,4-Trichloro-1,3- cyclopentenedione	591-35-5 88552- 47-0	60	N.D.	✓	N.D.
29	1,178.4	1-Methylene-1H-indene	2471-84- 3	128	✓	✓	N.D.
30	1,192.2	Acetophenone	98-86-2	105	N.D.	✓	N.D.
31	1,204.2	Benzoic acid	65-85-0	105	✓	✓	N.D.
32	1,243.2	2,2,4,5-tetrachlorocyclopent-4-ene- 1,3-dione	15743- 13-2	87	✓	✓	N.D.
33	1,249.8	Benzoic acid, 4-chloro	74-11-3	139	N.D.	✓	N.D.
34	1,273.2 1,287.6 1,326	Benzaldehyde, 2,3- dichloro or Benzaldehyde, 2,4- dichloro or Benzaldehyde, 2,6-dichloro or Benzaldehyde, 3,4-dichloro or Benzaldehyde, 3,5-dichloro	6334-18- 5 874-42-0 83-38-5 6287-38- 3 10203- 08-4	139	✓	N.D.	N.D.
35	1,282.2	Benzofuran, 5,7-dichloro	23145- 06-4	168	N.D.	✓	N.D.
36	1,299.6	2,6-Dichlorostyrene or 3,4-Dichlorostyrene	28469- 92-3 2039-83- 0	137	✓	✓	N.D.
37	1,309.2 1,386	Acetophenone, 2-chloro- or Ethanone, 2-(formyloxy)-1-phenyl	532-27-4 55153- 12-3	105	✓	✓	N.D.
38	1,339.8	Naphalene, methyl	90-12-0	142	✓	✓	N.D.
39	1,355.4	Phthalic anhydride	85-44-9	104	✓	✓	N.D.
40	1,353 1,357.2 1,415.4	Benzene, 1,2,3,4-tetrachloro or Benzene, 1,2,3,5-tetrachloro or Benzene, 1,2,4,5-tetrachloro	634-66-2 634-90-2 95-94-3	216	✓	✓	N.D.
41	1,364.4 1,638	2,3,6-Trichlorophenol or 3,4,5-Trichlorophenol	933-75-5 609-19-8	196	N.D.	N.D.	N.D.
42	1,373.4	2-Chloro-1,4-dihydroxybenzene	615-67-8	144	✓	✓	N.D.
43	1,388.4	2,3,6-Trichlorophenol	933-75-5	196	✓	✓	N.D.
44	1,424.4	Biphenyl	92-52-4	154	✓	✓	✓
45	1,452.6	1-Naphtalenol, 4-chloro	604-44-4	178	✓	✓	N.D.
46	1,467.6	2,3,5-Trichlorobenzaldehyde or 2,3,6-Trichlorobenzaldehyde	56961- 75-2 4659-47- 6	207	N.D.	N.D.	N.D.
47	1,479.6 1,540.8 1,552.2	Diphenylmethane or 2-Methylbiphenyl or 3-Methylbiphenyl or 4-Methylbiphenyl	101-81-5 643-58-3 643-93-6 644-08-6	168	✓	✓	N.D.
48	1,572.6	Pentachlorobenzene	608-93-5	250	✓	✓	N.D.
49	1,543.8 1,599.6	2,4-Dichloro-1-naphthol or 3,4-Dichloro-1-naphthol	2050-76- 2 5728-20- 1	212	✓	✓	N.D.
50	1,576.2 1,777.8	2-Phenylphenol or 4-Phenylphenol or 3-Phenylphenol	90-43-7 92-69-3 580-51-8	170	✓	✓	N.D.
51	1,581.6	Dibenzofuran	132-64-9	168	✓	N.D.	N.D.
52	1,609.2	Phenylmaleic anhydride	36122- 35-7	102	✓	✓	N.D.
53	1,615.2	2,3,4,5-Tetrachlorophenol		232	✓	✓	N.D.

Table 2 (continued)

No.	t_R (s)	Compound	CAS No.	Base peak m/z	Long conditioning Tenax® GR	Long conditioning Tenax® TA	Compounds detected by SAM
			4901-51-3				
		2,3,4,6-Tetrachlorophenol	58-90-2				
		2,3,5,6-Tetrachlorophenol	935-95-5				
54	1,616.4	4-Chlorophthalic acid	89-20-3	138	✓	N.D.	N.D.
55	1,618.8	3,4,5-Trichlorocatechol	56961-20-7	212	✓	✓	N.D.
56	1,631.4	2-Chlorobiphenyl	2051-60-7	188	✓	N.D.	N.D.
		3-Chlorobiphenyl	2051-61-8				
		4-Chlorobiphenyl	20514-62-9				
57	1,650.6	Fluorene	86-73-7	166	✓	N.D.	N.D.
58	1,659.6	3-(4-Chlorophenyl)-2,5-furandione	3152-15-6	136	✓	✓	N.D.
59	1,677	Phenyl-4-cyclopentene-1,3-dione	51306-96-8	102	✓	N.D.	N.D.
60	1,685.4	9H-Fluoren-9-ol	1689-64-1	181	✓	N.D.	N.D.
61	1,687.8	Diphenylacetylene	501-65-5	178	N.D.	✓	N.D.
62	1,693.8	2,5-Cyclohexadiene-1,4-dione, 2-phenyl	363-03-1	184	✓	N.D.	N.D.
63	1,698	Benzophenone	119-61-9	105	✓	✓	N.D.
64	1,725	9-Methylene, 9H-Fluorene	4425-82-5	178	✓	✓	N.D.
65	1,767	Hexachlorobenzene	118-74-1	284	✓	✓	N.D.
66	1,777.8	<i>p</i> -Hydroxybiphenyl	92-69-3	170	✓	✓	N.D.
67	1,786.2	2-Hydroxy-5-chlorobiphenyl	607-12-5	204	✓	✓	N.D.
		4-Chloro-4'-hydroxybiphenyl	28034-99-3				
		2-Chloro-4-phenylphenol	92-04-6				
68	1,818	Pentachlorophenol	87-86-5	266	✓	✓	N.D.
69	1,829.4	2-Phenylindene	4505-48-0	192	✓	✓	N.D.
70	1,837.2	Tetrachlorohydroquinone	87-87-6	248	✓	✓	N.D.
71	1,892.4	[1,1'-Biphenyl]-2,5-diol	1079-21-6	186	✓	N.D.	N.D.
		[1,1'-Biphenyl]-4,4'-diol	92-88-6				
72	1,916.4	1-H-Indene, 1-(phenylmethylene)-	5394-84-5	203	✓	✓	N.D.
73	1,916.4	2-Phenylindane	35465-71-5	204	✓	✓	N.D.
74	1,927.8	4-Hydroxy-9-fluorenone	1986-00-1	196	N.D.	✓	N.D.
75	1,929.6	[1,1'-Biphenyl]-2-ol, 2',5'-dichloro	53905-30-9	238	✓	✓	N.D.
		[1,1'-Biphenyl]-3-ol, 2',5'-dichloro	53905-29-6				
		[1,1'-Biphenyl]-4-ol, 2',5'-dichloro	5335-24-0				
		[1,1'-Biphenyl]-4-ol, 3,4'-dichloro	53905-31-0				
		[1,1'-Biphenyl]-4-ol, 3,5-dichloro	1137-59-3				
76	1,930.8	2-Dibenzofuranol	86-77-1	184	✓	✓	N.D.
77	1,948.2	Dichlorodibenzofuran	5409-83-6	236	✓	✓	N.D.
78	1,968	5-Chloro-2-phenylbenzofuran		228	✓	✓	N.D.

Table 2 (continued)

No.	t_R (s)	Compound	CAS No.	Base peak m/z	Long conditioning Tenax® GR	Long conditioning Tenax® TA	Compounds detected by SAM
			18761-36-9				
		6-Chloro-2-phenylbenzofuran	4521-05-5				
		5-Chloro-3-phenylbenzofuran	54923-63-6				
79	2,126.4	2,3-Diphenylmaleic anhydride	4808-48-4	178	✓	✓	N.D.
80	2,157.6	<i>p</i> -Terphenyl	92-94-4	230	✓	✓	N.D.
	2,175.6	<i>m</i> -Terphenyl	92-06-8				
	2,199	<i>o</i> -Terphenyl	84-15-1				
81	2,184	2,3-5,6-Dibenzoxalene	243-24-3	218	✓	N.D.	N.D.
82	2,219.4	2,6-Diphenylphenol	2432-11-3	246	✓	✓	N.D.
	2,235						
83	2,293.8	Indeno[2,1b]oxine, 2-phenyl	10435-67-3	244	✓	✓	N.D.
	2,314.8	Dibenzofuran, 4-Phenyl	NA				
	2,326.8	Dibenzofuran, 1-Phenyl	NA				
84	2,308.8	2,4-Dichloro- <i>p</i> -terphenyl	61576-83-8	298	✓	✓	N.D.
85	2,311.8	4-Chloro- <i>p</i> -Terphenyl	1762-83-0	264	✓	✓	N.D.
86	2,376.6	2,5-Diphenyl-1,4-benzoquinone	844-51-9	102	✓	✓	N.D.
87	2,400	Cyclopent-2-enone	NA	279	✓	N.D.	N.D.
		5-benzylideno-3-(4-chlorophenyl)-					
88	2,455.2	Indeno[2,1b]pyran, 2-4-chlorophenyl-	62096-34-8	278	✓	✓	N.D.
89	2,707.2	<i>m</i> -Terphenyl, 5'phenyl	612-71-5	306	✓	✓	N.D.
	2,729.4	<i>m,m</i> -Quaterphenyl	1166-18-3				
		<i>m,p</i> -Quaterphenyl	1166-19-4				
		<i>o,o'</i> -Quaterphenyl	641-96-3				
		<i>p,p'</i> -Quaterphenyl	135-70-6				
		<i>o,p</i> -Quaterphenyl	1165-58-8				
90	2,761.8	2, 4, 6-Triphenylphenol	NA	322	✓	✓	N.D.
91	3,333.6	6,6-Diphenylfulvene	2175-90-8	230	N.D.	✓	N.D.

Note. They are presented with their retention times, their CAS numbers, and the base m/z peak of formation detected during experiments concerning the effect of perchlorates salt on the Tenax® adsorbents. A specific column corresponds to the compounds detected by SAM.

Abbreviations: ✓: detected compound; GC-MS: gas chromatograph mass spectrometer; N.D.: nondetected compound; SAM: Sample Analysis at Mars.

MTBSTFA is in contact with the Tenax®, we also studied the influence of the MTBSTFA alone versus an MTBSTFA/DMF mixture on the Tenax® GR trap as a function of the trap temperature (100 to 600 °C).

3.2.1. Tenax® and MTBSTFA By-Products

This first experiment placed 0.5 µl of MTBSTFA in contact with 10 mg of long-conditioned Tenax® to observe if the derivatization reagent had any impact on the degradation of Tenax® compared with thermal degradation only when the mixture is heated. The results are presented in Table 1. The heating of the mixture of MTBSTFA and Tenax® lead to the formation of several by-products of MTBSTFA and Tenax® (thermal degradation products and derivatized molecules).

Numerous MTBSTFA by-products, listed in Figure 11, were formed either by thermal degradation or by reaction with water (coming from the ambient atmosphere and from the sample). MTBSTFA dissociated to form 2,2,2-trifluoro-*N*-methyl-*N*-(trimethylsilyl)-acetamide (MSTFA); 2,2,-trifluoro-*N*-methyl-acetamide;

trimethylsilanol; 2,2,2-trifluoro-*N*-methylacetamide; trimethylsilanol; *tert*-butyldimethylsilanol; and 1,3-di-*tert*-butyl-1,1,3,3-tetramethyldisiloxane from 100 °C. In addition, two chemical products were formed as the result of the reaction of the acidic hydrogens of water with MTBSTFA: *tert*-butyldimethylsilanol (mono-silylated water) and 1,3-bis(1,1-dimethylethyl)-1,1,3,3-tetramethyldisiloxane (bi-silylated water).

Three other by-products were observed, *tert*-butyldimethylfluorosilane (TBDMS-F) above 350 °C, diphenyldifluorosilane above 350 °C, and tris (trimethylsilyl)borate above 100 °C. The detection of the TBDMS-F suggests the formation of hydrofluoric (HF) acid from the thermal degradation of MTBSTFA by-products (from 350 °C). Indeed, we observed that the abundance of 2,2,2-trifluoro-*N*-methyl-*N*-(trimethylsilyl)acetamide detected at 600 °C was half the abundance observed at 100 °C. This abundance decrease can be explained by the reactivity of the MTBSTFA and the thermal degradation of MTBSTFA by-products, which increase with the temperature, leading to the quantitative increase of silylated water compounds and to the production of other by-products including HF (see Figure 12). We did not observe the presence of HF (pKa=3.2) by GC-MS because this compound was too much reactive to be detected, having been derivatized to form *tert*-butyldimethylfluorosilane. We also note that SAM GC-MS analysis results also indicate the production of TBDMS-F.

To explain the formation of the diphenyldifluorosilane, we investigated two possible pathways of production. First, we surmised that the diphenyldifluorosilane production could potentially occur through the reaction of HF with diphenyl polysiloxane (from the stationary phase of the column), but this reaction is only possible if a catalyst (e.g., CuF₂) is used (Kim & Sieburth, 2007). However, the formation of diphenyldifluorosilane (Figure 13, right) could also be explained by the reaction between borosilicate glass, diphenyl polysiloxane from the stationary phase of the column, and MTBSTFA by-products. Borosilicate glass (mostly composed of SiO₂-B₂O₃) is widely used in chemistry laboratory glassware and was employed to carry the MTBSTFA. It has been demonstrated that the hydrolysis of the borosilicate glass (e.g., under the action of water) creates a layer of boric acid (H₃BO₃) on the surface of the glass (Bunker et al., 1986; George, 2015; Leippy et al., 2006; Peter et al., 2013). The formation of the boric acid has been confirmed in MTBSTFA derivatization experiments using borosilicate glass through the detection of derivatized boric acid (e.g., Brault, 2015; Elsila et al., 2008). The borosilicate glass structure was likely altered in contact with atmospheric water, leading to the formation of boric acid. Boric acid could have then reacted with HF formed at 350 °C to produce boron trifluoride (BF₃) and tetrafluoroboric acid HBF₄ (Brotherton et al., 2000). Finally, perfluorinated complex anions like BF₄⁻ are able to transform many polymers of cyclosiloxanes into diphenyldifluorosilane at 200 °C (Bulkowski et al., 1975; Farooq, 1997, 2000). Hence, diphenyldifluorosilane seems to be the result of the reaction between diphenyl polysiloxane and fluoroboric acid.

Concerning the tris(trimethylsilyl)borate, we suspect the boron atom originated from the borosilicate glass used to carry the MTBSTFA (Figure 13), as boric acid B(OH)₃ is produced from borosilicate glass. In addition, when boric acid is injected on a Restek Rtx-20 GC column, it reacted with the stationary phase made of 20% of diphenyl polysiloxane and 80% of dimethyl polysiloxane: tris (trimethylsilyl)borate may be thereby produced (Bünger & Zografou, 2014).

Compared to our experiment on the thermal degradation of long-conditioned Tenax® GR, only additional molecules, which do not originate directly from the degradation of MTBSTFA, were also formed when MTBSTFA is contacted with long conditioned Tenax (Figure 12). These include cresol, acetophenone, 3-phenyl-3-butene-2-one, 9-methylene 9H-fluorene, and 2,4,6-triphenylphenol. In addition, the alteration of the conditioned Tenax® GR appeared to be enhanced by the presence of MTBSTFA: the addition of MTBSTFA influences the temperature of release of Tenax® thermal degradation products. In other words, molecules tend to be formed at lower temperatures in the presence of MTBSTFA. This observation might be explained by the aggressive HF formed from the derivatization reagent, which is detected in its derivatized form TBDMS-F. Indeed, it should be noted that the increase in temperature from 100 to 600 °C increased the quantity of silylated HF and that the amount of HF formed could have participated in the degradation of Tenax® GR (Figure 12). Nevertheless, TBDMS-HF appears only at 350 °C, while the Tenax® degradation starts around 150 °C. Certainly, other mechanisms could stimulate Tenax® degradation in presence of MTBSTFA at lower temperature, but the nature of these processes remains difficult to determinate.

Thermal degradation products of Tenax® contain labile hydrogens (i.e., alcohol group), which make them able to react with MTBSTFA via a silylation reaction (i.e., 1-trimethylsilanol [pKa = 12.5], phenol

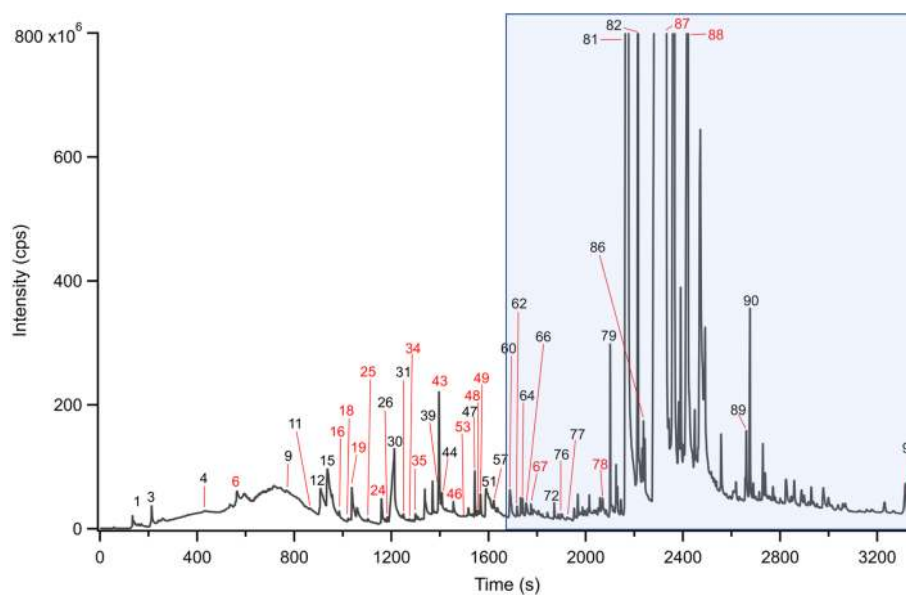


Figure 14. Chromatogram obtained on a RTX-5sil-MS (Restek) column after analysis of a mixture of 25 mg of Tenax® TA and 12 mg of calcium perchlorates (32wt%), without the additional oven, at 400 °C (the numbers correspond to those presented in Table 2). The compounds number in red correspond to chlorinated species. The shaded part corresponds to all the compounds unable to be seen by Sample Analysis at Mars due to their high retention times. Temperature program: 35 °C hold for 8 min then 7 °C/min up to 300 °C. Then isotherm at 300 °C for 10 min.

[pKa = 9.95], cresol [pKa ~10], and hydroxybiphenyl [pKa ~9]). Nevertheless, the only derivatized Tenax® by-product detected was TBDMS-benzoic acid formed between 250 and 600 °C (Table 1). The lack of detection of silylated alcohols could be explained by the low efficiency of the reaction of derivatization of alcohols. Indeed, with alcohol, even just 1% of *tert*-butyldimethylchlorosilane can act as a catalyzer (Orata, 2012). As the reactivity of alcohol with a silylation reagent follows the order of primary > secondary > tertiary, the reactivity of our alcohol could be decreasing as a result. Then, the detection of derivatized benzoic acid would result from better efficiency of the derivatization reaction of carboxylic acids compared to alcohols under the experimental conditions used or via the contamination of the sample, as the benzoic acid-TBDMS was detected in the blank but in smaller quantities.

3.2.2. Effect of MTBSTFA/DMF Mixtures on Tenax®

The results of the experiment of exposing Tenax® GR to 0.5 µl of a mixture MTBSTFA/DMF (4:1), at various temperatures, are presented in Table 1.

Adding DMF to MTBSTFA slightly decreased the temperature of Tenax® degradation and led to the production of fewer numbers of molecules from the Tenax® GR alteration compared to the previous experiment with MTBSTFA alone (Figure 12). For instance, the presence of DMF in the mixture inhibited the formation of compounds including fluorene, 4-methyl-2-phenylphenol, 4-phenyl-4-cyclopentene-1,3-dione, 9-methylene-9H-fluorene, 1-benzyl-naphthalene, and 2,4,6-triphenylphenol. The addition of DMF inhibited the impact of MTBSTFA degradation products on Tenax® GR. The polymer appears to be more thermally stable with DMF/MTBSTFA mixture instead of MTBSTFA alone, as its degradation started at 500 °C (versus 200–250 °C for Tenax® GR; see Table 1).

Previous studies using HF and DMF mixtures demonstrate that HF is more reactive in presence of aprotic solvents such as DMF or DMSO (dimethyl sulfoxide) (Harrasz et al., 2005; Kim et al., 2009). The aprotic solvent increases the dissociation reaction rate of HF, freeing then the anions (F⁻ and HF₂⁻) to react are free to react with Tenax® GR. However, this was opposite of the phenomenon we observed. These results may be because DMF supports the derivatization reaction (Buch et al., 2006), leading to a rise in the conversion of MTBSTFA into 2,2,2-trifluoro-*N*-methylacetamide and avoiding the formation of HF. This hypothesis was supported by the lack of detection of TBDMS-F during this experiment.

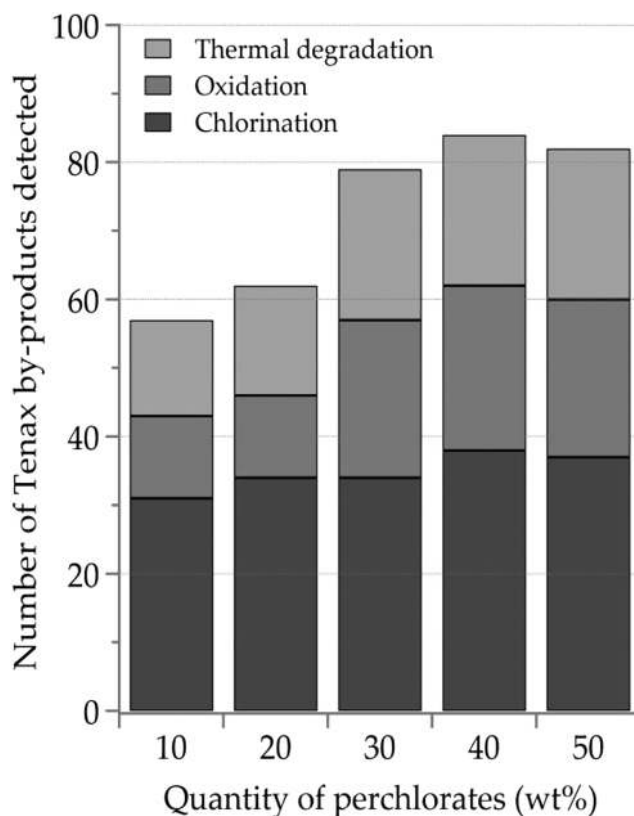


Figure 15. Number of molecules detected (above the three times the background noise level) by the gas chromatograph-mass spectrometer analysis of products released by thermal decomposition of Tenax® GR mixed with several amounts of calcium perchlorates at 400 °C. These products have been classified according to the thermal degradation products (light grey), oxidation (medium dark), and chlorination (dark grey).

3.3. Effect of Calcium Perchlorate Salts on Tenax® TA and GR

3.3.1. Tenax® and Calcium Perchlorates By-Products

The presence of perchlorates and chlorates in the Martian soil has been established at several places on Mars. In order to observe and list all the potential by product of the reaction of perchlorate on Tenax® we have used much more perchlorate than the amount detected on Mars.

Calcium perchlorate salts are decomposed during soil pyrolysis. When they are heated, they are decomposed to form calcium chloride (CaCl₂). Then, at high temperature, in contact with water, the CaCl₂ is transformed into HCl (Glavin et al., 2013; Migdał-Mikuli & Hetmańczyk, 2008) as described below:



Adapted from Glavin et al. (2013) and Migdał-Mikuli and Hetmańczyk (2008).

The presence of O₂ and HCl trigger the Deacon reaction, which produces chlorine (Cl₂) and H₂O (Jarmohamed & Mulder, 1983; Lewis, 1906; Magistro & Cowfer, 1986).



These by-products of perchlorates have an impact on the degradation products of Tenax®. In the course of the Tenax® and perchlorates direct contact experiments at 400 °C, 30 oxidized molecules and 39 chemical species

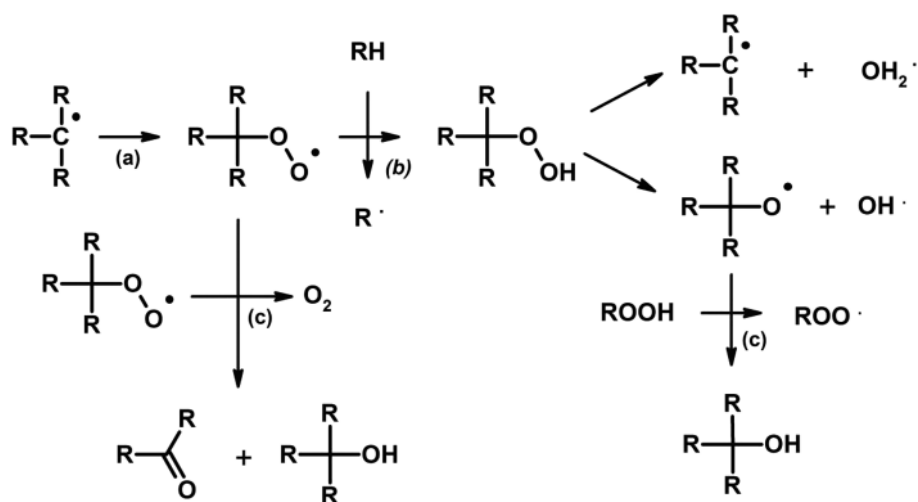


Figure 16. Mechanism of degradation of organic matter due to the presence of oxygen, which leads to an increase of the propagation of the degradation (a) and to the production of alcohols, carbonyls (b), and phenylperoxy radical (c).

containing chlorine were detected in addition to 22 products from thermal degradation. From the literature, no HCl is observed at lower temperatures than 450 °C (equation 3) when pure calcium perchlorate is heated alone (Cannon et al., 2012; Migdał-Mikuli & Hetmańczyk, 2008; Sutter et al., 2015). Here, however, we observe chlorination of Tenax® at lower temperature. The difference with simple degradation of Ca-perchlorate is that in our experiments we have complex organic compounds (Tenax®) present, which can slightly change the release temperature of HCl in presence of water, shifting it at lower temperature. This, for example, is the case when we compare the O₂ releasing peak from lab to the O₂ released peak from SAM experiment at Gale Crater (Sutter et al., 2015).

The list of all molecules detected in the experiments performed on the chemical reactivity of Tenax® in direct contact with calcium perchlorates is shown in Table 2.

Figure 14 shows a chromatogram of the analysis of 25 mg of Tenax® TA mixed with 12 mg of Ca (ClO₄)₂ (~32wt%).

During this experiment, a mixture of Tenax® and perchlorates was heated to 400 °C, a higher temperature than used in SAM (300 °C), in order to observe Tenax® and calcium perchlorate by-products (Table 2). There were three groups of compounds generated by the degradation of Tenax® GR in the presence of calcium perchlorates: Tenax® GR degradation by-products, oxidized molecules and chlorinated compounds. Figure 15 shows the evolution of the number of Tenax® by-products, above the 3 times the background noise level, as a function of the amount of perchlorates. The more perchlorates there were, the more we observed by-products from the degradation of Tenax® GR. This observation is explained by both the catalysis of the initiation and propagation of Tenax® GR degradation by perchlorate degradation products and by their reactivity with Tenax® GR by-products.

As seen previously, decomposition products are not only released by the simple decomposition of Tenax®. They could also come from the degradation of the polymer propagated due to the presence of oxygen. Without O₂, the propagation of degradation occurred through hydrogen transfer or depolymerization. With O₂, peroxy radicals formed (Figure 16a), which supported the propagation of polymer degradation (Figure 16b) (Ilie & Senetscu, 2009; Yousif & Haddad, 2013). Finally, this decomposition of Tenax® GR led to the formation of molecules by polymer degradation propagation due to the presence of O₂ (e.g., benzene) as well as the oxidation of compounds that contain oxygen atoms (e.g., benzoic acid).

In the experiments, we also observed molecules formed by the oxidation of Tenax® degradation products, including alcohols, aldehydes, carboxylic acids, and ethers. The oxidation by O₂ formed peroxy radical from Tenax® polymer that initiated the formation of molecules with alcohol and carbonyl groups as shown on

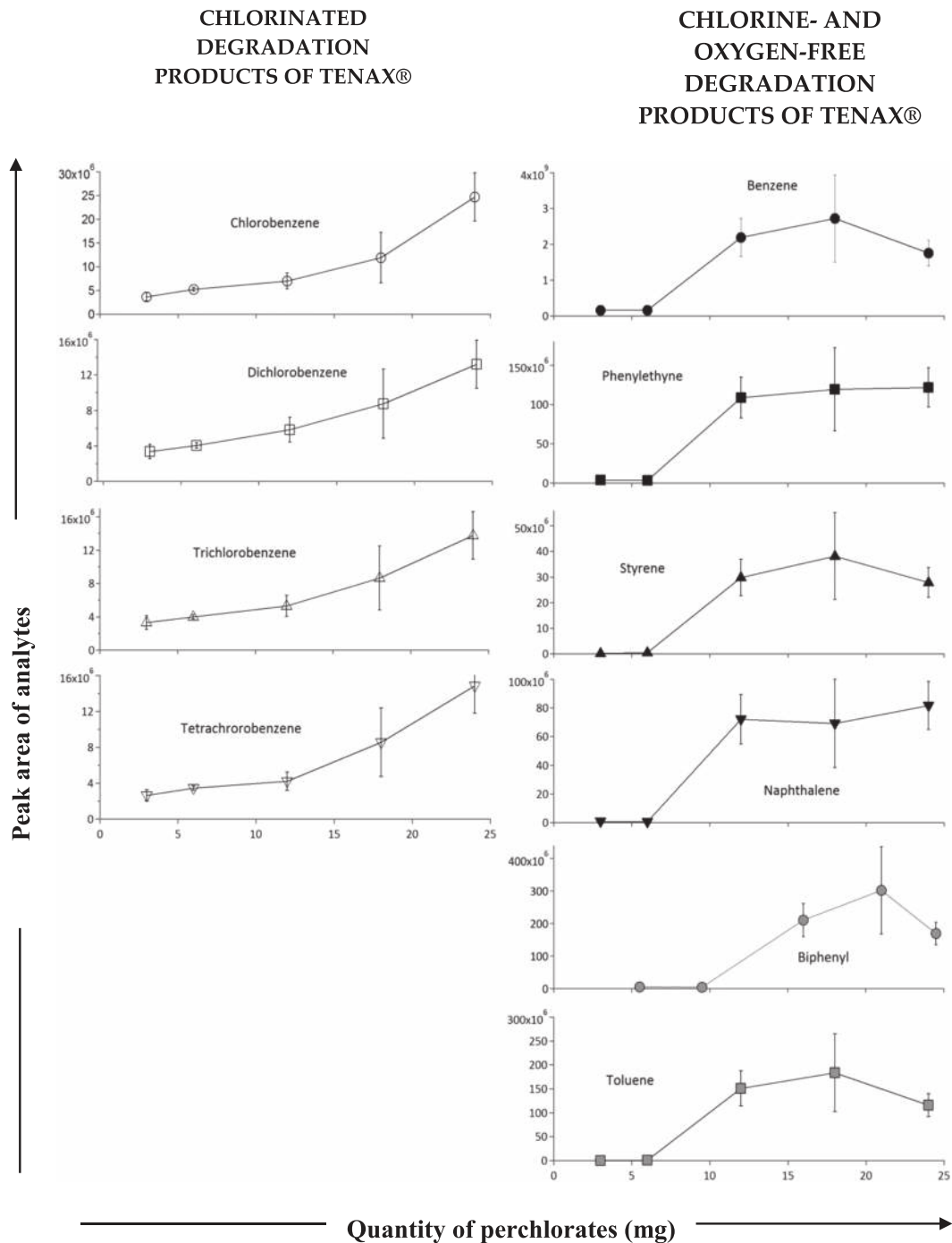


Figure 17. Evolution with the amount of perchlorate of the quantity of Tenax® GR degradation products (medium grey) and chlorinated products (black). Benzene (m/z 78), toluene (m/z 91), phenylethyne (m/z 102), styrene (m/z 104), naphthalene (m/z 128) and biphenyl (m/z 154) /chlorobenzene (m/z 112), dichlorobenzene (m/z 146), trichlorobenzene (m/z 182), and tetrachlorobenzene (m/z 216).

Figure 16c (Ilie & Senetscu, 2009). Oxidation may have also targeted alcohol and the carbonyl groups: carboxylic acid can be obtained from ketone oxidation, for instance. Cyclization processes can also generate ethers from alkyloxy radicals.

Chlorinated compounds were generated either by chlorination through hydrochloric acid (addition of the chlorine atoms from HCl) or by chlorine (chlorine atoms from Cl_2 which is formed by the reverse Deacon reaction or from the recombination of chloride radicals; equation (4)). Indeed, in addition, the presence of

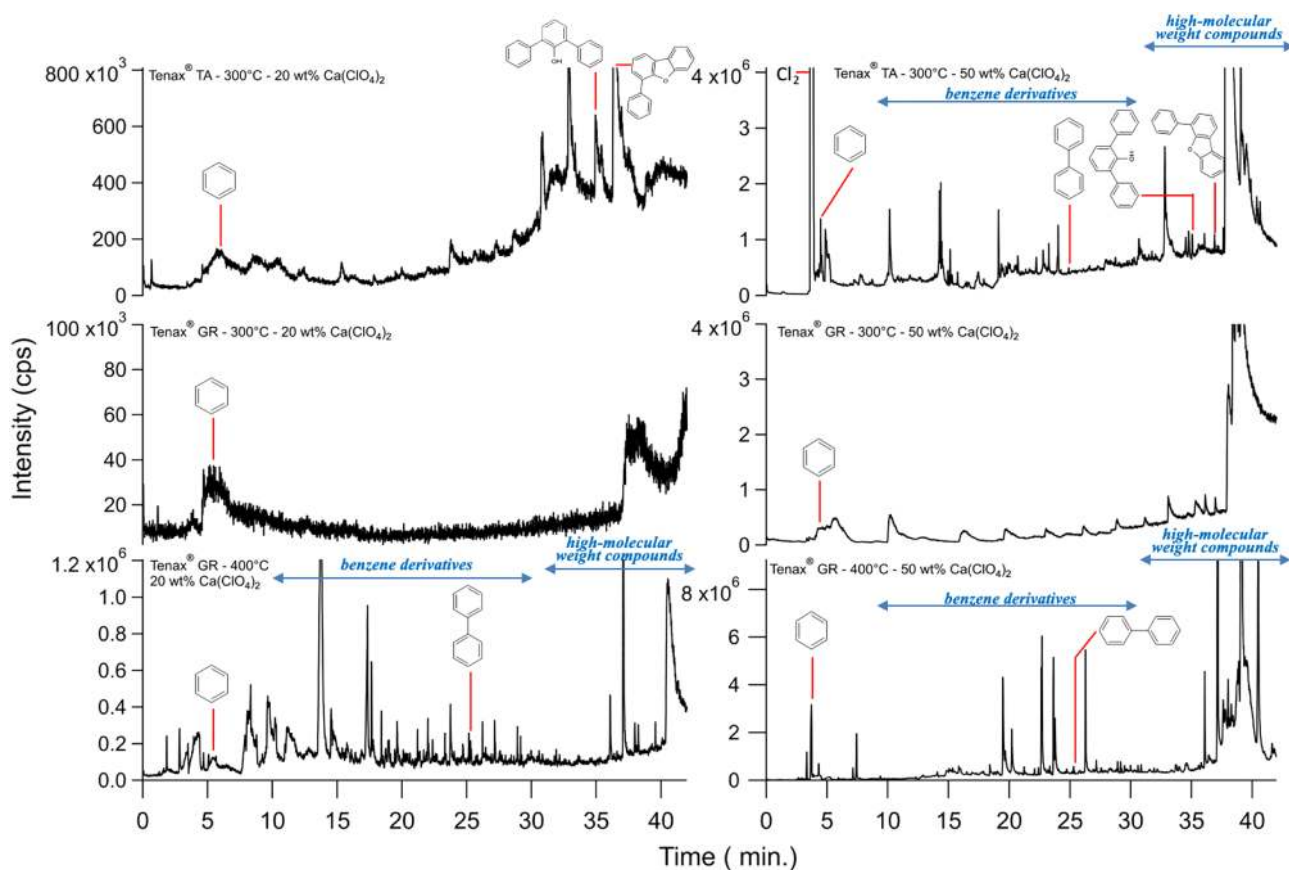


Figure 18. Chromatograms, with a RTX-5SilMS column, showing the compounds release by Tenax® GR and Tenax® TA (25 mg) when they were heated at 300 or 400 °C in presence of perchlorates (~6 and 25 mg which is equal to 20 and 50 wt% of Tenax® quantity) Cl₂ (*m/z* 70), benzene (*m/z* 78), biphenyl (*m/z* 154), *m*-terphenyl-2'-ol (*m/z* 246), phenyldibenzofuran (*m/z* 244). Temperature program: 35 °C hold for 8 min then 7 °C/min up to 300 °C then isotherm at 300 °C for 10 min.

Cl₂ could support the initiation of the degradation of Tenax® (Pellizzari et al., 1984). The chlorination by-products of Tenax® GR included chlorinated phenyl molecules, chlorobenzaldehyde, chlorophthalic acid, chlorobiphenyl, chlorinated phenol, chlorinated benzenediol, chlorinated benzofuran, and chlorinated dibenzofuran.

Figure 17 shows the relative quantity of Tenax® by-products as a function of the abundance of perchlorate salts. The effect of perchlorates on Tenax® GR is reflected by the increase of benzene, toluene, phenylethyne, styrene, naphthalene, and biphenyl as perchlorate increases. These quantities increased dramatically above 19 wt% of perchlorates and continue to increase before declining or balancing at approximately 42 wt%. The increase in quantity of unchlorinated Tenax® GR by-products at low perchlorate amount (below ~42 wt %) shows that the perchlorates support the propagation of Tenax® degradation. Nevertheless, below ~42 wt% of salt, the oxidation and chlorination were predominant, which is why unchlorinated and unoxidized Tenax® GR by-products decrease (Figure 15).

The abundance of chlorinated phenyl compounds (i.e., chlorobenzene, dichlorobenzene, trichlorobenzene, and tetrachlorobenzene) increased with the mixing ratio of perchlorates for the entire range of abundances investigated (Figure 17). We assume that this evolution by a rise of the rate of chlorination and oxidation agents that both triggered the degradation of Tenax® and intensified the chlorination and the oxidation of Tenax®. Among arenes (aromatic HCs) derivatives formed from the decomposition of Tenax®, there were potential chlorobenzene precursors. For instance, carbonyl compounds (e.g., benzoic acid) are subjected to decarboxylation (Steininger et al., 2012; Wim & Robert, 1978) followed by chlorination addition, forming

chlorinated benzene derivatives. In addition, diphenyl and terphenyl derivatives and even Tenax[®] polymer (by side chain elimination) can release a phenyl radical or phenylperoxyl radical (in presence of O₂; Figure 16) with which react the chlorination agents (HCl or Cl₂) (Born et al., 1993; de Mey & Kooyman, 1971). Chlorine radicals could also initiate the chlorination reaction. Indeed, the oxychlorination (i.e., the action of O₂ and HCl or Cl₂) of chlorobenzene lead to the production of polychlorinated phenyl molecules as dichlorobenzene, trichlorobenzene, tetrachlorobenzene, polychlorinated dibenzofurans, polychlorinated biphenyls, and polychlorinated phenol (Sommeling et al., 1994; Wim & Robert, 1978). All of those compounds were detected in our experiments, thus resulting from the oxychlorination of chlorinated compounds. From a quantitative point of view, it is important to note that dichlorobenzene, trichlorobenzene, and tetrachlorobenzene are in the same range of abundance. This is atypical but not surprising. Indeed, it has been showed that the distribution of the chlorophenyl is a function of several parameters, including the percentage of perchlorate, and the nature and the amount of the organic matter, which reacts with perchlorate (Millan, 2016; Miller et al., 2015). In addition, experiments have shown that benzene, toluene, benzoic acid, phthalic acid, and mellitic acid, when in contact with calcium perchlorate, can generate chlorobenzene, dichlorobenzene, trichlorobenzene, and tetrachlorobenzene (Miller et al., 2015). Thus, the diversity of the by-products of the Tenax[®] trap could explain the high abundance of the polychlorophenyl compounds.

3.4. SAM Analogue Experiments

SAM analogue experiments used an additional reactor (Figure 3), which allowed us to heat perchlorates separately from the Tenax[®] to mimic the SAM experiments. Several experiments with differing amounts of calcium perchlorate (up to 50wt%) placed in the reactor and heated to 400 °C were ran. The gaseous degradation products of perchlorates were sent to the GC injector, where 25 mg of Tenax[®] TA or GR had been cooled to 0 °C and then heated to 300 or 400 °C.

For perchlorate contents up to 50 wt% and a Tenax[®] temperature of 300 °C, observed the formation of benzene, m-terphenyl-2'-ol/m-terphenyl-4'-ol and 4-phenyldibenzofuran, which was formed directly from Tenax[®] by random-chain scission and side chain elimination. The increase in either perchlorate or temperature induced the production of new Tenax[®] by-products similar to those detected in our direct contact experiments. Benzene derivatives (e.g., benzene, benzaldehyde, benzoic acid, chlorobenzene, and dichlorobenzene), biphenyl, and high-molecular weight compounds (e.g., terphenyl, m-terphenyl-2'-ol, phenyldibenzofuran, 2,6-diphenyl-p-benzoquinone) were also detected.

We found that the formation of Tenax[®] by-products was affected by the quantity of perchlorates, the type of Tenax[®] (GR or TA), and the exposure temperature of Tenax[®] (Figure 18). The rise of perchlorate quantity was accompanied by the quantitative and qualitative growth of Tenax by-products. This observation is consistent with direct contact experiment results. Oxygen and hydrochloric acid supported the propagation of the Tenax[®] decomposition and amplified the formation of Tenax[®] by-products.

The comparison of Tenax[®] GR and Tenax[®] TA results all show that Tenax[®] TA releases more compounds when exposed to O₂ and HCl. This can be explained by a simple quantitative effect as there is a higher fraction of PPPO polymer in Tenax[®] TA (30%) for a given mass adsorbent compared to Tenax[®] GR. The graphite present in Tenax[®] GR can also possibly play a role by absorbing more heat than PPPO, thus limiting the temperature reached by the PPPO compared to Tenax[®] TA within the same operating conditions.

Finally, we found that the maximum temperature Tenax[®] is heated had a strong influence on Tenax[®] by-product production: the higher the Tenax[®] temperature, the more products were generated from thermal decomposition, oxidation, and chlorination of the adsorbents.

3.5. Discussions Regarding the Results From the SAM Experiment

Our experiments shed light on the mechanism of production of some SAM analytes (i.e., tris (trimethylsilyl) borate, TBDMS-F and TBDMS-phenol) as well as the factors that may have influenced the formation of Tenax[®] by-products during SAM experiments.

3.5.1. Production Mechanisms of Certain SAM Analytes

The formation of tris (trimethylsilyl)borate was initiated by the hydrolysis of borosilicate glass exposed to ambient environment, which led to the production of boric acid. In our experiments, when boric acid was injected in the GC-5 MTX CLP column (made of cyanopropylphenyl dimethyl polysiloxane), it interacted

with the dimethylpolysiloxane of the stationary phase to form tris(trimethylsilyl)borate. On SAM, boric acid should originate from the MTBSTFA/DMF mixture prepared in glass vials prior to be conditioned in the SAM SMS or from the glass beads used in the HC trap. As the MTBSTFA conditioning vessel from Sigma-Aldrich was made of class III hydrolytic glass, it does not contain borosilicate and is not at the origin of tris(trimethylsilyl)borate.

TBDMS-F originates from the MTSBTFA derivatization of HF, a MTBSTFA degradation product. The derivatization reaction and the MTSBTFA decomposition are concurrent: when the derivatization reaction is not fostered (e.g., in absence of DMF), the MTBSTFA may be decomposed into TBDMS-F. Inversely, the MTBSTFA involved in the derivatization reaction does not decompose and does not produce TBDMS-F. Concerning SAM, some nanomoles of TBDMS-F were detected (between 0.5 and 3.7 nmol) for almost all the sample analyses with the exception of Rocknest-3 and Cumberland-blank 2 (Stern et al., 2015). This detection of TBDMS-F suggests a decomposition of MTBSTFA in absence of DMF, which as a lower boiling point than MTBSTFA.

The TBDMS-phenol is the derivatized form of phenol, which is the only Tenax[®] by-product that has been derivatized. Phenol is one of the chemical species the most likely to be silylated (in order of reactivity to silylation: alcohol > phenol > carboxyl > amine > amide/hydroxyl) (Orata, 2012).

3.5.2. Analytical Bias Induced by Using Tenax[®] Adsorbents on SAM

The main sources of analytical bias induced by Tenax[®] are due to (1) the release of Tenax[®] manufacturing residues; (2) the release of small size fragment of Tenax[®]; (3) adsorbent decomposition, notably when it is brought about by analytes; and (4) the release of analytes, which persist within the adsorbent. Then, the purpose of conditioning is to remove artifacts to avoid analytical bias. During the SAM integration phase, SAM traps were cleaned. Thus, some sources of Tenax[®] by-products were removed, such as Tenax[®] manufacturing residues.

To limit the presence of Tenax[®] by-products, the adsorbents were tentatively isolated from the ambient atmosphere in order to limit the formation of new adsorbent residues to the minimum (Maurizio et al., 1992), but this was not possible for the years they were stored in the laboratory before the MSL launch. Then, a reactivation of the SAM adsorbents could explain the detection of Tenax[®] by-products. Despite the blank used to clean the trap (Tdesorption~300 °C, helium flow 0.03 atm.cc/s (Mahaffy et al., 2012), it appears likely that this was not enough to efficiently remove all the Tenax[®] by-products and other analytes that could have persisted on the traps. However, only a small fraction of the by-products compounds coming from Tenax[®] itself are detected by SAM, i.e., seven aromatic compounds over 31 by-products: benzene, toluene, ethylbenzene, styrene, phenol, naphthalene, and biphenyl (Table 1). The other degradation compounds are not detected by SAM mainly because there are produced at temperatures higher than the SAM trap temperature of release, but also because some by-products are too heavy (not volatile and thermally stable at that temperature) to be eluted within the SAM's chromatographic conditions (type of the chromatographic column, He flow, and temperature ramp).

SAM results reveal the detection of Tenax[®]-induced aromatic molecule, yet the SAM trap desorption temperature is below the temperature of Tenax[®] by-products formation (400 °C) we found during our experiments. Thus, additional factors have to be taken in consideration to explain the Tenax[®]-induced aromatic molecules detected by SAM, such as conditioning, the influence of MTBSTFA/DMF, the presence of perchlorates, and the aging of the Tenax[®] with the cycling of temperature.

Laboratory experiments tend to demonstrate a correlation between MTBSTFA decomposition and the increase of Tenax[®] alteration. On SAM, TBDMS-F detection suggests that a fraction of MTBSTFA has been decomposed. Thus, the alteration of SAM Tenax[®] trap may have been intensified by MTBSTFA by-products.

From a qualitative point of view, adjunction of MTBSTFA on Tenax[®] produces 10 new by-products, which are mainly generated from the thermal degradation of MTBSTFA. Among them, eight by-products are detected by SAM and very well-known. Three of them are derivatized compounds originating from free water and from a carboxylic acid which is generated from Tenax[®] degradation (benzoic acid).

The more recent results show that the highest concentration of perchlorate is located at Yellowknife bay (Gale crater) in the Cumberland sample. This perchlorate concentration is about 1.05 ± 0.44 wt % (Sutter

et al., 2017), which is equivalent to a total amount of 1.42 ± 0.59 mg of ClO_4 in the triple portion of Cumberland. In this study the first by-product compounds are observed from 3 mg of perchlorate. Compared to the list of by-products generated by Tenax[®] (Tables 1 and 2), only three supplementary compounds are observed by SAM: two chlorinated compounds (chlorobenzene and dichlorobenzene) and one nonchlorinated compound (xylene). However, based on our laboratory results, we note that the amount of perchlorate in the Mars' soil at Gale Crater and the temperature of the trap release (300 °C) do not justify the detection of Tenax[®] by-products under SAM experimental conditions. However, the age and different cycles of Tenax[®] combined with the presence of perchlorate could explain the presence of these compounds in the background noise of SAM. Those facts reinforce that the detection of chlorobenzene by SAM at Cumberland place is endogenous to the sample and not due to the reaction of perchlorate and Tenax[®].

4. Conclusions

We found that Tenax[®] TA and GR both start to decompose around 400 °C and that Tenax[®] thermal degradation leads to the formation of phenyl, biphenyl, and terphenyl derivatives. Yet the starting temperature of Tenax[®] degradation is 100 °C above the desorption temperature of SAM trap.

To explain the detection of Tenax[®] by-products from SAM trap, we investigated other factors that could affect the stability of the Tenax[®] adsorbent. We discovered that conditioning influenced artifact production. Tenax[®] adsorbents release artifacts, including Tenax[®] manufacturing residues, persistent analytes within the adsorbent, and Tenax[®] by-products. Thus, it is necessary to condition the adsorbents with heating under gas flow to remove those artefacts.

We also observed a correlation between MTBSTFA decomposition and the intensification of MTSBTFA-soaked Tenax[®]. The addition of DMF to MTBSTFA supports a derivatization reaction, which reduces the impact of MTBSTFA on Tenax[®].

Regarding experiments with calcium perchlorates and Tenax[®], contact of perchlorate decomposition products and Tenax[®] during desorption propagate Tenax[®] decomposition and can cause the formation of new Tenax[®] by-products (notably oxidized and chlorinated compounds). SAM analogue experiments showed that the formation of Tenax[®] by-products induced by the presence of perchlorates by-products was influenced by the quantity of perchlorates, the type of Tenax[®], and the desorption temperature.

Lastly, we note that Tenax[®] TA is more vulnerable than Tenax[®] GR to thermal degradation and perchlorates effects, explained by the higher fraction of PPPO polymer and higher specific area of Tenax[®] TA.

In summary, we conclude that the production of by-products in the SAM trap may be caused by insufficient conditioning, the presence of MTBSTFA, and by the overheating or aging of the adsorbent. We also conclude that we have proved that the presence of chlorobenzene and dichlorobenzene at Cumberland place is not due to the reaction of Tenax[®] with perchlorate.

Acknowledgments

The SAM gas chromatograph is funded by the French space agency Centre National d'Etudes Spatiales. R. Navarro Gonzalez has received funds from the Universidad Nacional Autónoma de México (PAPIIT IN111619). Data used for the results of this paper are available at this address: <https://doi.org/10.17632/ncwpcgcj7x.2>.

References

- Archer, P. D., Franz, H. B., Sutter, B., Arevalo, R. D. Jr., Coll, P., Eigenbrode, J. L., et al. (2014). Abundances and implications of volatile-bearing species from evolved gas analysis of the Rocknest aeolian deposit, Gale Crater, Mars. *Journal of Geophysical Research: Planets*, *119*, 237–254. <https://doi.org/10.1002/2013JE004493>
- Benner, S. A., Devnne, K. G., Matveeva, L. N., & Powel, D. H. (2000). The missing organic molecules on Mars. *PNAS*, *97*(6).
- Biemann, K., Oro, J., Toulmin, P. 3rd, Orgel, L. E., Nier, A. O., Anderson, D. M., et al. (1976). Search for organic and volatile inorganic compounds in two surface samples from the chryse planitia region of Mars. *Science (New York, N.Y.)*, *194*(4260), 72–76. <https://doi.org/10.1126/science.194.4260.72>
- Biemann, K., Oro, P., Nier, A. O., Anderson, D. M., Simmonds, P. G., Flory, D., et al. (1977). The search for organic substances and inorganic volatile compounds in the surface of Mars. *Journal of Geophysical Research*, *82*(28), 4641–4658. <https://doi.org/10.1029/JG082i028p04641>
- Bittner, J. D., & Howard, J. B. (1981). Composition profiles and reaction mechanisms in a near-sooting premixed benzene/oxygen/argon flame. *Symposium (International) on Combustion*, *18*(1), 1105–1116. [https://doi.org/10.1016/S0082-0784\(81\)80115-4](https://doi.org/10.1016/S0082-0784(81)80115-4)
- Born, J. G. P., van der Wart, H. W. A., Mulder, P., & Louw, R. (1993). Gas-phase oxychlorination of benzene. *Recueil des Travaux Chimiques des Pays-Bas*, *112*(4), 262–270. <https://doi.org/10.1002/recl.19931120405>
- Brault, A. (2015). Study of the efficiency of amino acid derivatization with MTBSTFA after acid hydrolysis and in analogues of various martian mineral matrices: Application to the Sample Analysis at Mars (SAM) and Mars Organic Molecule Analyzer (MOMA) experiments, Ecole Centrale Paris.
- Brotherton, R. J., Weber, C. J., Guibert, C. R., & Little, J. L. (2000). Boron compounds. In *Ullmann's Encyclopedia of Industrial Chemistry*, *6*, 237–258. Wiley-VCH. https://doi.org/10.1002/14356007.a04_309

- Buch, A., Glavin, D. P., Sternberg, R., Szopa, C., Rodier, C., Navarro-González, R., et al. (2006). A new extraction technique for in situ analyses of amino and carboxylic acids on Mars by gas chromatography mass spectrometry. *Planetary and Space Science*, *54*(15), 1592–1599. <https://doi.org/10.1016/j.pss.2006.05.041>
- Buch, A., Sternberg, R., & Chazalnoel, P. (2009). In C. N. d. E. Spatiales (Ed.), *Device for preparing and injecting a sample*. Dispositif de préparation et de Focalisation d'échantillons. Patent N° 107173/FR.
- Buch, A., Sternberg, R., Szopa, C., Freissinet, C., Garnier, C., Bekri, E. J., et al. (2009). Development of a gas chromatography compatible Sample Processing System (SPS) for the in-situ analysis of refractory organic matter in martian soil: Preliminary results. *Advances in Space Research*, *43*(1), 143–151. <https://doi.org/10.1016/j.asr.2008.05.001>
- Bulkowski, J. E., Stacy, R., & Van Dyke, C. H. (1975). The interaction of organosilanes with triphenylmethyl tetrafluoroborate. *Journal of Organometallic Chemistry*, *87*(2), 137–143. [https://doi.org/10.1016/S0022-328X\(00\)91280-4](https://doi.org/10.1016/S0022-328X(00)91280-4)
- Bünger, D., & Zografou, I. (2014). Method for producing a non-Newtonian fluid in particular for impact protection, Method for producing an impact protection by means of a non-Newtonian fluid, Impact protection by means of a non-Newtonian fluid, and Object with such impact protection, edited, German.
- Bunker, B. C., Arnold, G. W., Day, D. E., & Bray, P. J. (1986). The effect of molecular structure on borosilicate glass leaching. *Journal of Non-Crystalline Solids*, *87*(1), 226–253. [https://doi.org/10.1016/S0022-3093\(86\)80080-1](https://doi.org/10.1016/S0022-3093(86)80080-1)
- Burns, E. A., & Muraca, R. F. (1962). Karl Fischer determination of water in ammonium perchlorate with automatic titration apparatus. Evaluation of Reaction Rate Parameters and Statistical Evaluation. *Analytical Chemistry*, *34*(7), 848–854. <https://doi.org/10.1021/ac60187a040>
- Cannon, K. M., Sutter, B., Ming, D. W., Boynton, W. V., & Quinn, R. (2012). Perchlorate induced low temperature carbonate decomposition in the Mars Phoenix Thermal and Evolved Gas Analyzer (TEGA). *Geophysical Research Letters*, *39*, L13203. <https://doi.org/10.1029/2012GL051952>
- Cao, X.-L., & Hewitt, C. N. (1994). Study of the degradation by ozone of adsorbents and of hydrocarbons adsorbed during the passive sampling of air. *Environmental Science & Technology*, *28*(5), 757–762. <https://doi.org/10.1021/es00054a003>
- Carrier, L. B., & Kounaves, P. S. (2015). The origins of perchlorate in the Martian soil. *Geophysical Research Letters*, *42*, 3739–3745. <https://doi.org/10.1002/2015GL064290>
- Challinor, J. M. (2001). Review: the development and applications of thermally assisted hydrolysis and methylation reactions. *Journal of Analytical and Applied Pyrolysis*, *61*(1-2), 3–34. [https://doi.org/10.1016/S0165-2370\(01\)00146-2](https://doi.org/10.1016/S0165-2370(01)00146-2)
- Chu, L., Deng, S., Zhao, R., Deng, J., & Kang, X. (2016). Comparison of adsorption/desorption of volatile organic compounds (VOCs) on electrospun nanofibers with Tenax TA for potential application in sampling. *PLoS ONE*, *11*(10), e0163388. <https://doi.org/10.1371/journal.pone.0163388>
- Clark, B. C., & Kounaves, S. P. (2016). Evidence for the distribution of perchlorates on Mars. *International Journal of Astrobiology*, *15*(4), 311–318. <https://doi.org/10.1017/S1473550415000385>
- Clausen, P. A., & Wolkoff, P. (1997). Degradation products of Tenax TA formed during sampling and thermal desorption analysis: Indicators of reactive species indoors. *Atmospheric Environment*, *31*(5), 715–725. [https://doi.org/10.1016/S1352-2310\(96\)00230-0](https://doi.org/10.1016/S1352-2310(96)00230-0)
- Colket, M. B., & Seery, D. J. (1994). Reaction mechanisms for toluene pyrolysis. *Symposium (International) on Combustion*, *25*(1), 883–891. [https://doi.org/10.1016/S0082-0784\(06\)80723-X](https://doi.org/10.1016/S0082-0784(06)80723-X)
- de Mey, C. A., & Kooyman, E. C. (1971). The halogenation of aromatics: Part X. Vapour phase chlorination of biphenyl. *Recueil des Travaux Chimiques des Pays-Bas*, *90*(12), 1337–1342. <https://doi.org/10.1002/recl.19710901210>
- Elsila, J. E., Stern, J. C., Glavin, D. P., & Dworkin, J. P. (2008). Compound-specific isotope analysis of amino acids for stardust-returned samples, in *39th Lunar and Planetary Science Conference*, edited, p. Abstract #2004, Lunar and Planetary Institute, Houston.
- Farooq, O. (1997). Nucleophilic fluorination of alkoxysilane with alkali metal hexafluorophosphate—Part 1. *Journal of Fluorine Chemistry*, *86*(2), 189–197. [https://doi.org/10.1016/S0022-1139\(97\)00112-7](https://doi.org/10.1016/S0022-1139(97)00112-7)
- Farooq, O. (2000). Fluoridative degradation of cyclosiloxanes with alkali metal salts of perfluorinated complex anion. Part 5. *Journal of Organometallic Chemistry*, *613*(2), 239–243. [https://doi.org/10.1016/S0022-328X\(00\)00537-4](https://doi.org/10.1016/S0022-328X(00)00537-4)
- Freissinet, C., Buch, A., Sternberg, R., Szopa, C., Geffroy-Rodier, C., Jelinek, C., & Stambouli, M. (2010). Search for evidence of life in space: Analysis of enantiomeric organic molecules by N,N-dimethylformamide dimethylacetal derivative dependant Gas Chromatography-Mass Spectrometry. *Journal of Chromatography A*, *1217*(5), 731–740. <https://doi.org/10.1016/j.chroma.2009.11.009>
- Freissinet, C., Glavin, D. P., Mahaffy, P. R., Miller, K. E., Eigenbrode, J. L., Summons, R. E., et al., & the MSL Science Team (2015). Organic molecules in the Sheepbed Mudstone, Gale Crater, Mars. *Journal of Geophysical Research: Planets*, *120*, 495–514. <https://doi.org/10.1002/2014JE004737>
- Frenklach, M., Clary, D. W., Gardiner, W. C., & Stein, S. E. (1985). Detailed kinetic modeling of soot formation in shock-tube pyrolysis of acetylene. *Symposium (International) on Combustion*, *20*(1), 887–901. [https://doi.org/10.1016/S0082-0784\(85\)80578-6](https://doi.org/10.1016/S0082-0784(85)80578-6)
- Gallois, N., Templier, J. L., & Derenne, S. (2010). Limitations in interpreting TMAH thermochemistry of natural organic matter via consideration of glycine and alanine derivatives. *Organic Geochemistry*, *41*(12), 1338–1340. <https://doi.org/10.1016/j.orggeochem.2010.05.018>
- Gaur, U., & Wunderlich, B. (1981). Heat capacity and other thermodynamic properties of linear macromolecules. III. Polyoxides. *Journal of Physical and Chemical Reference Data*, *10*(4), 1001–1049. <https://doi.org/10.1063/1.555649>
- Geffroy-Rodier, C., Grasset, L., Sternberg, R., Buch, A., & Amblès, A. (2009). Thermochemistry in search for organics in extraterrestrial environments. *Journal of Analytical and Applied Pyrolysis*, *85*(1-2), 454–459. <https://doi.org/10.1016/j.jaap.2008.10.005>
- George, J. L. (2015). Dissolution of borate glasses and precipitation of phosphate compounds, 176 pp, Missouri University of Science and Technology.
- Glavin, D. P., Freissinet, C., Miller, K. E., Eigenbrode, J. L., Brunner, A. E., Buch, A., et al. (2013). Evidence for perchlorates and the origin of chlorinated hydrocarbons detected by SAM at the Rocknest aeolian deposit in Gale Crater. *Journal of Geophysical Research: Planets*, *118*, 1955–1973. <https://doi.org/10.1002/jgre.20144>
- Goesmann, F., Brinckerhoff, W. B., Raulin, F., Goetz, W., Danell, R. M., Getty, S. A., et al. (2017). The Mars Organic Molecule Analyzer (MOMA) instrument: Characterization of organic material in martian sediments. *Astrobiology*, *17*(6-7), 655–685. <https://doi.org/10.1089/ast.2016.1551>
- Goetz, W., Brinckerhoff, W. B., Arevalo, R. Jr., Freissinet, C., Getty, S., Glavin, D. P., et al. (2016). MOMA: the challenge to search for organics and biosignatures on Mars. *International Journal of Astrobiology*, *15*(3), 239–250. <https://doi.org/10.1017/s1473550416000227>
- Guzman, M., McKay, C. P., Quinn, R. C., Szopa, C., Davila, A. F., Navarro-González, R., & Freissinet, C. (2018). Identification of chlorobenzene in the Viking gas chromatograph-mass spectrometer data sets: reanalysis of Viking mission data consistent with aromatic organic compounds on Mars. *Journal of Geophysical Research: Planets*, *123*, 1674–1683. <https://doi.org/10.1029/2018JE005544>

- Hamins, A. P. (1993). Soot. In I. K. Puri (Ed.), *environmental Implication of Combustion Process* (pp. 71–95). Boca Raton, FL: CRC Press.
- Harraz, F. A., Kamada, K., Kobayashi, K., Sakka, T., & Ogata, Y. H. (2005). Random macropore formation in p-type silicon in HF-containing organic solutions: Host matrix for metal deposition. *Journal of the Electrochemical Society*, *152*(4), C213–C220. <https://doi.org/10.1149/1.1864292>
- Hecht, M. H., Kounaves, S. P., Quinn, R. C., West, S. J., Young, S. M. M., Ming, D. W., et al. (2009). Detection of perchlorate and the soluble chemistry of martian soil at the Phoenix Lander Site. *Science (New York, N.Y.)*, *325*(5936), 64–67. <https://doi.org/10.1126/science.1172466>
- Ilie, S., & Senetscu, R. (2009). Polymeric Materials review on oxidation, stabilization and evaluation using CL and DSC MethodsRep., 1-62 pp.
- Jarmohamed, W., & Mulder, P. (1983). Chapter XXV: The oxychlorination of organic substances. In G. I. Golodets (Ed.), *Studies in Surface Science and Catalysis* (pp. 793–797). Amsterdam – Oxford – New-York: Elsevier. [https://doi.org/10.1016/S0167-2991\(08\)64850-8](https://doi.org/10.1016/S0167-2991(08)64850-8)
- Kataoka, H. (1996). Derivatization reactions for the determination of amines by gas chromatography and their applications in environmental analysis. *Journal of Chromatography A*, *733*(1), 19–34. [https://doi.org/10.1016/0021-9673\(95\)00726-1](https://doi.org/10.1016/0021-9673(95)00726-1)
- Kim, J. K., & Sieburth, S. M. (2007). Diphenyldifluorosilane, in *Encyclopedia of Reagents for Organic Synthesis*. New-York: edited, <https://doi.org/10.1002/9780470842898.rm00725>
- Kim, K. P., Kim, H. K., Lyu, S. H., Woo, H. S. S., & Lee, J. H. (2009). Three-dimensional macropore arrays in p-type silicon fabricated by electrochemical etching. *Journal of the Korean Physical Society*, *55*(1). <https://doi.org/10.3970/cmc.2012.031.147>
- Kleno, J. G., Wolkoff, P., Clausen, P. A., Wilkins, C. K., & Pedersen, T. (2002). Degradation of the adsorbent Tenax TA by nitrogen oxides, ozone, hydrogen peroxide, OH radical, and limonene oxidation products. *Environmental Science & Technology*, *36*(19), 4121–4126. <https://doi.org/10.1021/es025680f>
- Lee, J. H., Batterman, S. A., Jia, C., & Chernyak, S. (2006). Ozone artifacts and carbonyl measurements using Tenax GR, Tenax TA, Carboxpack B, and Carboxpack X adsorbents. *Journal of the Air & Waste Management Association*, *56*(11), 1503–1517.
- Leipply, D., Melhus, B. A., Leonardo, M. R., Feller, S. A., & Affatigato, M. (2006). Development of functional borate glass surfaces to inhibit bacterial growth. *Glass Technology - European Journal of Glass Science and Technology Part A*, *47*(5), 127–132.
- Leshin, L. A., Mahaffy, P. R., Webster, C. R., Cabane, M., Coll, P., Conrad, P. G., et al. (2013). Volatile, isotope, and organic analysis of Martian fines with the Mars Curiosity Rover. *Science (New York, N.Y.)*, *341*(6153), 1238937. <https://doi.org/10.1126/science.1238937>
- Lewis, G. N. (1906). Equilibrium in the Deacon process. *Journal of the American Chemical Society*, *28*(10), 1380–1395. <https://doi.org/10.1021/ja01976a008>
- Lin, D.-L., Wang, S.-M., Wu, C.-H., Chen, B.-G., & Liu, R. (2008). Chemical derivatization for the analysis of drugs by GC-MS—A conceptual review. *Journal of Food and Drug Analysis*, *16*, 1–10.
- Magistro, A. J., & Cowfer, J. A. (1986). Oxychlorination of ethylene. *Journal of Chemical Education*, *63*(12), 1056. <https://doi.org/10.1021/ed063p1056>
- Mahaffy, P., Webster, C. R., Cabane, M., Conrad, P. G., Coll, P., Atreya, S. K., et al. (2012). The Sample Analysis at Mars Investigation and Instrument Suite. *Space Science Reviews*, *170*(1-4), 401–478. <https://doi.org/10.1007/s11214-012-9879-z>
- Masonjones, M. C., Mukherjee, J., Sarofim, A. F., Taghizadeh, K., & Lafleur, A. L. (1996). High temperature pyrolysis of O-terphenyl: Evidence for kinetic control in the benzene polymerization pathway and importance of arene aggregation/condensation reactions in the formation of polycyclic aromatic hydrocarbons. *Polycyclic Aromatic Compounds*, *8*(4), 229–242. <https://doi.org/10.1080/10406639608048350>
- Maurizio, B., Helmut, K., Emilio, P., Herbert, S., & Henk, V. (1992). Comparison of Tenax and carbotrap for VOC sampling in indoor Air. *Indoor Air*, *2*(4), 216–224. <https://doi.org/10.1111/j.1600-0668.1992.00004.x>
- Migdal-Mikuli, A., & Hetmańczyk, J. (2008). Thermal behavior of [Ca(H₂O)₄](ClO₄)₂ and [Ca (NH₃)₆](ClO₄)₂. *Journal of Thermal Analysis and Calorimetry*, *91*(2), 529–534. <https://doi.org/10.1007/s10973-007-8511-z>
- Millan, M. (2016). Etude de la composition de la surface de Mars: recherche de molécules organiques par analyse physico-chimique in situ avec l'instrument SAM de la mission Mars Science Laboratory.
- Miller, K., Eigenbrode, J. L., Freissinet, C., Glavin, D. P., Kotrc, B., Francois, P., & Summons, R. E. (2016). Potential precursor compounds for chlorohydrocarbons detected in Gale Crater, Mars, by the SAM instrument suite on the Curiosity Rover. *Journal of Geophysical Research: Planets*, *121*, 296–308. <https://doi.org/10.1002/2015JE004939>
- Miller, K., Kotrc, B., Summons, R. E., Belmahdi, I., Buch, A., Eigenbrode, J. L., et al. (2015). Evaluation of the Tenax trap in the Sample Analysis at Mars instrument suite on the Curiosity rover as a potential hydrocarbon source for chlorinated organics detected in Gale Crater. *Journal of Geophysical Research: Planets*, *120*, 1446–1459. <https://doi.org/10.1002/2015JE004825>
- Ming, D. W., Archer, P. D., Glavin, D. P., Eigenbrode, J. L., Franz, H. B., Sutter, B., et al. (2014). Volatile and organic compositions of sedimentary rocks in Yellowknife Bay, Gale Crater, Mars. *Science (New York, N.Y.)*, *343*(6169), 1245267. <https://doi.org/10.1126/science.1245267>
- Moldoveanu, S. C. (1998). Chapter 15. Analytical pyrolysis of other natural organic polymers. In S. C. Moldoveanu (Ed.), *Techniques and Instrumentation in Analytical Chemistry* (pp. 435–437). Amsterdam: Elsevier. [https://doi.org/10.1016/S0167-9244\(98\)80036-X](https://doi.org/10.1016/S0167-9244(98)80036-X)
- Moldoveanu, S. C., & David, V. (2002). Chapter 20—Chemical degradation of polymers and pyrolysis. In C. M. Serban, & D. Victor (Eds.), *Journal of Chromatography Library* (pp. 847–917). Amsterdam: Elsevier. [https://doi.org/10.1016/S0301-4770\(02\)80021-5](https://doi.org/10.1016/S0301-4770(02)80021-5)
- NASW-4355, N. H. (1988). Lesson learned from the Viking planetary quarantine and contamination control experienceRep., NASA.
- Navarro-Gonzalez, R., Vargas, E., de la Rosa, J., Raga, A. C., & McKay, C. P. (2010). Reanalysis of the Viking results suggests perchlorate and organics at midlatitudes on Mars. *Journal of Geophysical Research*, *115*, E12010. <https://doi.org/10.1029/2010JE003599>
- Omidvarborna, H., Kumar, A., & Kim, D.-S. (2015). Recent studies on soot modeling for diesel combustion. *Renewable and Sustainable Energy Reviews*, *48*, 635–647. <https://doi.org/10.1016/j.rser.2015.04.019>
- Orata, F. (2012). *Derivatization reactions and reagents for gas chromatography analysis*. Rijeka, Croatia and Shanghai, China: INTECH Open Access Publisher.
- Pellizzari, E., Demian, B., & Krost, K. (1984). Sampling of organic compounds in the presence of reactive inorganic gases with Tenax GC. *Analytical Chemistry*, *56*(4), 793–798. <https://doi.org/10.1021/ac00268a046>
- Peter, Z., Haiying, H., D, K. K., & J, C. L. (2013). First-principles study of hydrolysis reaction barriers in a sodium borosilicate glass. *International Journal of Applied Glass Science*, *4*(4), 395–407. <https://doi.org/10.1111/ijag.12052>
- Poch, O., Kaci, S., Stalport, F., Szopa, C., & Coll, P. (2014). Laboratory insights into the chemical and kinetic evolution of several organic molecules under simulated Mars surface UV radiation conditions. *Icarus*, *242*, 50–63. <https://doi.org/10.1016/j.icarus.2014.07.014>
- Shadkani, F., & Helleur, R. (2010). Recent applications in analytical thermochemistry. *Journal of Analytical and Applied Pyrolysis*, *89*(1), 2–16. <https://doi.org/10.1016/j.jaap.2010.05.007>
- Sichina, W. J. (2011). Characterization of polymers using TGARep.

- Silverman, L., Trego, K., Houk, W., & Shideler, M. E. (2007). The pyrolysis of p-terphenyl: Separation and identification of the thermal products. *Journal of Applied Chemistry*, 8(9), 616–624. <https://doi.org/10.1002/jctb.5010080914>
- Sommeling, P. M., Mulder, P., & Louw, R. (1994). Formation of PCDFs during chlorination and oxidation of chlorobenzene in chlorine/oxygen mixtures around 340 °C. *Chemosphere*, 29(9), 2015–2018. [https://doi.org/10.1016/0045-6535\(94\)90368-9](https://doi.org/10.1016/0045-6535(94)90368-9)
- Stalport, F., Coll, P., Szopa, C., Cottin, H., & Raulin, F. (2009). Investigating the photostability of carboxylic acids exposed to Mars surface ultraviolet radiation conditions. *Astrobiology*, 9(6), 543–549. <https://doi.org/10.1089/ast.2008.0300>
- Stalport, F., Guan, Y. Y., Coll, P., Szopa, C., Macari, F., Raulin, F., et al. (2010). UVolution, a photochemistry experiment in low earth orbit: Investigation of the photostability of carboxylic acids exposed to mars surface UV radiation conditions. *Astrobiology*, 10(4), 449–461. <https://doi.org/10.1089/ast.2009.0413>
- Steininger, H., Goesmann, F., & Goetz, W. (2012). Influence of magnesium perchlorate on the pyrolysis of organic compounds in Mars analogue soils. *Planetary and Space Science*, 71(1), 9–17. <https://doi.org/10.1016/j.pss.2012.06.015>
- Stern, J. C., Sutter, B., Freissinet, C., Navarro-González, R., McKay, C. P., Archer, P. D. Jr., et al. (2015). Evidence for indigenous nitrogen in sedimentary and aeolian deposits from the Curiosity rover investigations at Gale crater, Mars. *Proceedings of the National Academy of Sciences*, 112(14), 4245–4250. <https://doi.org/10.1073/pnas.1420932112>
- Sutter, B., Heil, E. C., Morris, R. V., Archer, P. D., Ming, D. W., Niles, P. B., et al. (2015). The investigation of perchlorate/iron phase mixtures as a possible source of oxygen detected by the Sample Analysis at Mars (SAM) instrument in Gale crater, Mars, in *46th Lunar and Planetary Science Conference*, edited, p. Abstract #2137, Lunar and Planetary Institute, Houston.
- Sutter, B., McAdam, A. C., Mahaffy, P. R., Ming, D. W., Edgett, K. S., Rampe, E. B., et al. (2017). Evolved gas analyses of sedimentary rocks and eolian sediment in Gale Crater, Mars: Results of the Curiosity rover's sample analysis at Mars instrument from Yellowknife Bay to the Namib Dune. *Journal of Geophysical Research: Planets*, 122, 2574–2609. <https://doi.org/10.1002/2016JE005225>
- Szopa, C., Freissinet, C., Glavin, D. P., Buch, A., Coll, P. J., Cabane, M., et al. (2015). Mars organic matter revealed by the detection of organo-chlorinated molecules from Pyro-GCMS analyses of Yellowknife Bay Mudstone, in *AGU Fall Meeting 2015*, edited, pp. P33A-2125, San Francisco, United States.
- Wampler, T. P. (2006). *Applied Pyrolysis Handbook*. Boca Raton: CRC Press.
- Webster, C. R., Mahaffy, P. R., Atreya, S. K., Moores, J. E., Flesch, G. J., Malespin, C., et al. (2018). Background levels of methane in Mars' atmosphere show strong seasonal variations. *Science (New York, N.Y.)*, 360(6393), 1093–1096. <https://doi.org/10.1126/science.aag0131>
- Weyland, H. G., Hoftyzer, P. J., & Van Krevelen, D. W. (1970). Prediction of the glass transition temperature of polymers. *Polymer*, 11(2), 79–87. [https://doi.org/10.1016/0032-3861\(70\)90028-5](https://doi.org/10.1016/0032-3861(70)90028-5)
- Wim, D., & Robert, L. (1978). The mechanism of the vapor-phase chlorination of benzene derivatives. *International Journal of Chemical Kinetics*, 10(3), 249–275. <https://doi.org/10.1002/kin.550100304>
- Witkowski, A., Stec, A. A., & Hull, T. R. (2016). Thermal decomposition of polymeric materials. In M. J. Hurley, D. Gottuk, J. R. Hall, K. Harada, E. Kuligowski, M. Puchovsky, J. Torero, J. M. Watts, & C. Wiczorek (Eds.), *SFPE handbook of fire protection engineering* (pp. 167–254). New York, NY: Springer New York. https://doi.org/10.1007/978-1-4939-2565-0_7
- Wrasidlo, W. (1971). Transitions and relaxations in Poly(2,6-diphenyl 1,4-phenylene ether). *Macromolecules*, 4(5), 642–648. <https://doi.org/10.1021/ma60023a027>
- Yousif, E., & Haddad, R. (2013). Photodegradation and photostabilization of polymers, especially polystyrene: review. *Springerplus*, 2(1), 398. <https://doi.org/10.1186/2193-1801-2-398>